

HAMILTON STANDARD
DIVISION OF UNITED AIRCRAFT CORPORATION
WINDSOR LOCKS, CONNECTICUT

FACILITY FORM 502

68-84124

(ACCESSION NUMBER)

(THRU)

114

(PAGES)

(CODE)

CR-65991

(NASA CR OR TAX OR AD NUMBER)

(CATEGORY)

POROUS PLATE WATER BOILER DESIGN STUDY

FINAL REPORT

May 20, 1965



Prepared by:

Joseph Sangiovanni
J. Sangiovanni

Senior Analytical Engineer

P. H. Kepner
P. H. Kepner

Analytical Engineer

Approved by:

John L. Warner
J. L. Warner

Head, Thermodynamic Analysis

TABLE OF CONTENTS

	<u>Page No.</u>
1.0 SUMMARY -----	1
2.0 CONCLUSIONS -----	3
3.0 RECOMMENDATIONS -----	5
4.0 INTRODUCTION -----	6
5.0 DISCUSSION OF COOLING MODES -----	9
5.1 Sublimation Mechanism -----	9
5.2 Evaporation Mechanism -----	11
5.3 Mixed Mode -----	12
6.0 SELECTION OF POROUS PLATE -----	14
6.1 Porous Structure -----	14
6.1.1 Pore Geometry -----	15
6.2 Material -----	17
6.2.1 Thermal Conductivity -----	17
6.2.2 Corrosion Resistance -----	18
6.2.3 Wettability -----	19
6.2.4 Other Material Considerations -----	20
7.0 MATHEMATICAL MODELS -----	22
7.1 Sublimation Mechanism -----	22
7.2 Evaporation Mechanism -----	23
7.3 Mixed Mode -----	25
7.4 Free Molecule Flow Through Porous Media ---	27
8.0 DISCUSSION OF TEST RESULTS -----	30
8.1 Performance Modes -----	30
8.2 Effects of Plate Characteristics -----	32
9.0 CONFIGURATIONS FOR TRANSPORT FLUID COOLING -----	35

TABLE OF CONTENTS

(continued)

	<u>Page No.</u>
APPENDIX A SAMPLE CALCULATIONS FOR THE GLYCOL HEATED MODULE #136X-54	41
APPENDIX B ILLUSTRATIONS	47
APPENDIX C PLATE CHARACTERISTICS AND PERFORMANCE DATA	66
APPENDIX D EXPERIMENTAL APPARATUS	81
APPENDIX E ANALYSIS OF THE SUBLIMATION MECHANISM WITH ENERGY TRANSFER BY CONDUCTION AND CONVECTION	95
SYMBOLS	101

LIST OF FIGURES

<u>Figure No.</u>	<u>Title</u>	<u>Page No.</u>
1	Typical Porous Plate Water Boiler for Transport Fluid Cooling	48
2.	Equilibrium Phase Diagram for Water	49
3	Comparison of Continuum Flow and Free Molecule Flow for Plate C	50
4	Some Alternate Arrangements of Regularly Packed Spheres	51
5	Model for Analysis of Sublimation Mechanism	52
6	Comparison of Measured Ice Layer Thickness and Heat Rejection Performance with Theoretical Predictions for Plate E Operating in the Sublimation Mode	53
7	Porous Plate Flow Characteristics at Simulated Operating Conditions -- Exit Pressures of 90 to 1500 Microns of Mercury	54
8	Comparison of Measured and Predicted Evaporation Heat Transfer Performance for Plate C	55
9	Comparison of Measured and Predicted Heat Transfer Performance of Plate C Operating in the Mixed Mode	56
10	Reproducibility of Heat Transfer Performance for Porous Plates Made to Identical Specifications	57
11 ^c	Effect of Plate Characteristics on Performance	58
12	Photograph of a Glycol Heated Porous Plate Water Boiler Test Module (Negative #S-37894)	59
13	Measured Performance of Glycol Heated Test Module No. 136X-52	60
14	Measured Performance of Glycol Heated Test Module No. 136X-53	61
15	Measured Performance of Glycol Heated Test Module No. 136X-54	62
16	Measured Performance of Glycol Heated Test Module No. 136X-55	63
17	Permsability of Nickel Porous Plate Q at Exit Pressures of 200-1500 Microns of Mercury	75

LIST OF FIGURES (Continued)

<u>Figure No.</u>	<u>Title</u>	<u>Page No.</u>
18	Permeability of Nickel Porous Plates Before and After Degradation in Performance Tests	76
19	Schematic of Vacuum System	86
20	Schematic of Water Feed Circuit	87
21	Schematic of AC Power Analyzer	88
22	Schematic of Glycol Circuit	89
23	Photograph of Entire Test Facility (Negative # G27262)	90
24	Photograph of Electrically Heated Test Module Set up in Vacuum Chamber (Negative #G27263)	91
25	Apparatus for Flow Testing Porous Plates (Negative # G27264)	92
26	Photograph of Electrically Heated Test Module (Negative #S-37893)	93
27	Photograph of Electrically Heated Test Module -- Exploded View (Negative #S-37895)	94
 <u>Drawing No.</u>		
136X-52-55	Glycol Test Modules (Sheet 1)	103
136X-52-55	Glycol Test Modules (Sheet 2)	104

LIST OF TABLES

<u>Table No.</u>	<u>Title</u>	<u>Page No.</u>
1	Bubble Point and Water Retention Pressures Before and After Degradation Tests	64
2	Performance of Porous Plates During Degradation Tests	64
3	Run Sequence Compared to Effectiveness Level	65
4	Average Effectiveness for Glycol Heated Modules	65
5	Performance of Phase IV Plates in Electrically Heated Modules	65
6	Description of Porous Plates	67
7	Measured Water Retention, Bubble Point, and Permeability of Porous Plates Used	68
8	Summary of Performance Data for Phase II Verification of Cooling Mechanisms	69
9	Summary of Performance Data for Phase III - Influence of Plate Variable	70
10	Analysis of Distilled Water Before Used in the Various Degradation Tests	77
11	Analysis of Water After Used in Degradation Tests	77
12	Performance Data Phase IV - Transport Fluid Heated Modules	78

1.0 SUMMARY

This study program was conducted to obtain a sound theoretical understanding of and a valid analytical method for predicting the performance of porous plate water boilers.

In the first of the four phases into which this program was divided, several model configurations were studied theoretically to provide the guidance for the comprehensive exploratory investigations to follow. Test equipment was designed and constructed and the experimental work was begun.

During Phase II, experimental efforts were directed towards establishing and identifying the cooling modes. These were identified as: 1) evaporation mode; 2) sublimation mode and; 3) mixed mode. The first two of these, which had been postulated previously in Phase I, were thus confirmed. Existence of the mixed mode, consisting of simultaneous operation in modes one and two, was discovered. Analytical methods were developed for predicting the performance in each of these modes and correlation of these results showed the importance of understanding the flow characteristics of the porous plate when discharging to vacuum ambients.

An experimental investigation of porous plate characteristics was conducted in Phase III, covering the heat flux range of operation to be encountered in current applications. As an addition to the original planning, the performance with time of porous plates made from sintered nickel particles was investigated

1.0 Continued.

and the cause of a performance degradation was established.

Modules representative of forthcoming applications for cooling of transport fluids were investigated in Phase IV in contrast to the electrically heated modules used in the earlier phases. Full use was made of the previously developed theory to guide this phase of the work. Four different modules were designed to focus on specific technical issues which might be peculiar to fluid heated units.

Work accomplished in Phases I through III has been comprehensively covered in previously submitted reports HSER 2942, HSER 2997, HSER 3183, and HSER 3314. The work done in Phase IV is covered by this report and detailed discussion of the important findings of the earlier phases is also included.

2.0 CONCLUSIONS

This program achieved its principal objective of defining the cooling mechanisms and developing a method for predicting the performance of porous plate water boilers. Performance calculation methods developed previously were successfully applied to a transport fluid heated module of conventional design. The primary conclusions drawn from the results of the program are as follows:

- 1) Mixed mode operation will be encountered in most current applications.
- 2) Pore size distribution is significant in the mixed mode requiring that the utmost care be used to define and to select suitable material. Flow and bubble point tests may have to be augmented to obtain adequate definition of a suitable plate.
- 3) Performance required for present missions can be met. However, the potential for pore blockage must be dealt with during design; in particular, allowance must be provided for the tendency of nickel plates in contact with water to form nickel hydroxide and hydrated nickel oxide.
- 4) Water retention of currently available sintered metal particle plates is insufficient to withstand feed pressures being considered for space vehicle applications (5-6 psia) when the ambient pressure is above the triple point pressure. Mixed mode operation is necessary to provide freezing in the larger pores and thereby prevent breakthrough and water carryover.

2.0 Continued

- 5) The mechanism of liquid breakthrough has been defined; however, its prediction requires a detailed knowledge of the pore size distribution and wettability of the porous structure.
- 6) Porous plate design must include consideration for the structural requirements imposed on plate areas by handling, manufacturing and the operational environment.
- 7) Performance was not degraded by brazing fins to the porous plate and blocking some of the pores.

3.0

RECOMMENDATIONS

An investigation of other potentially suitable porous plate structures besides sintered metal powders is recommended.

From the theory developed in this report other materials and pore structures can be expected to exhibit adequate ability to satisfy thermal requirements. Such an evaluation might show that a change in material or structure would give improved performance for less weight and for longer mission cycles.

Alternate materials and surface treatments offer potential advantages to operation in the evaporation mode. This mode was shown to exist at high heat fluxes where a correspondingly high sink temperature exists. To make use of this mode, higher fluid retention pressures are required but surface properties and pore size control these pressure levels. Thus an increase in the scope of materials engineering work could be beneficial and additional studies in this area are recommended.

4.0 INTRODUCTION

It is common practice to transfer heat from a heat source -- such as personnel or electronic equipment -- to a transport fluid, and convey this fluid to a convenient location where the heat is rejected. In an adaptation of this concept peculiar to space vehicles, the ultimate discharge of heat to space vacuum is accomplished by means of a porous plate boiler, which is a unique device for the full utilization of the heat of sublimation and/or evaporation of a pure substance. This device is ideally suited for short space missions where an expendable fluid, such as water, can be used for cooling. No flow control or valve is needed to modulate the coolant flow from a pressurized supply tank because it is self-regulating with heat dissipation requirements. Various configurations of the device can be used, depending on the cooling required. Figure 1 shows one configuration which has been used for cooling a transport fluid, the construction of which is typical of compact heat exchanger designs for aerospace applications. The expendable fluid section of this device is the portion on which the efforts of this investigation were concentrated. This section comprises a porous plate, a finned fluid passage, and the necessary headers.

The design function of the porous plate water boiler is to provide cooling by expending a medium at a suitable temperature level. The fluid expended is discharged to the surrounding ambient as a vapor, at a temperature level determined by the saturation

4.0 Continued.

pressure characteristics of the substance used. Water exhausting to a vacuum (50-500 μ Hg) was used as the working substance and ambient pressure for these investigations, but the device is not limited in this respect. The only requirements are that it must be possible to feed the substance to be expended into the boiler in a liquid state, and the ambient pressure must be suitable for evaporating or sublimating the fluid. The primary factor in determining the usefulness of a particular substance in a given application is the sink temperature -- the temperature of this substance at the sublimation/evaporation interface -- produced in conjunction with the surrounding ambient. It is this sink level that provides the potential for heat transfer from the transport fluid or heat source and thus defines the heat rejection capability. While the ultimate sink temperature is related to the ambient pressure, it was found in the early phases of development of this device that, because a vapor pressure drop existed due to the porous plate, the low temperature corresponding to the ambient pressure (vacuum) was not available as a sink.

The basic objectives of this investigation were a theoretical understanding of the mechanism by which cooling is produced, and a definition of the operating limits, porous material characteristics, and configurations suitable for cooling a transport fluid in space vehicle applications. It was found that there are two basic mechanisms by which evaporative cooling can occur when a porous plate is used in an expendable mass cooling device to separate the phase change substance from a lower pressure ambient.

4.0

Continued.

The two basic mechanisms were appropriately named the evaporation and sublimation mechanisms for the types of phase change involved. As might be expected, the particular characteristics of each mechanism are strongly dependent on the pore size. Since the pore size for most porous materials is non-uniform it is possible to have the device operating under both mechanisms simultaneously, and this is referred to as the mixed mode. The following discussions will show how it is possible for these two mechanisms to exist by themselves or simultaneously depending on the porous structure and operating conditions.

5.0 DISCUSSION OF COOLING MODES

5.1 Sublimation Mechanism

The sublimation mechanism is characterized by a layer of ice on the inside face of the porous plate, which prevents liquid from passing into the plate and escaping to the ambient. The existence of this ice layer is determined by a combination of the vapor pressure drop characteristics of the porous plate and the heat flux or vapor flow rate. When the vapor pressure drop of the porous plate is less than the triple point pressure indicated by the equilibrium diagram for the expendable substance (Figure 2) the phase change must be from the solid directly to the vapor phase, by sublimation of the ice layer. The thickness of the ice is governed by the rate of heat transfer and the sublimation temperature corresponding to the local vapor pressure at the inlet face of the porous plate. It can be shown that normal operating pressure differentials across the porous plate and ice layer are insufficient to extrude the ice into the pores and thus the ice forms a barrier to liquid flow into the pores. In order to accommodate the heat transfer requirement the ice sublimates at the porous plate face and freezes at a corresponding rate at the liquid interface. The ice therefore flows somewhat in the manner of a glacier toward the porous plate, but at an extremely slow rate while serving as a heat conduction media. This was actually observed by following small gas inclusions in the ice during visual tests of operating modules.

5.1 Continued.

For reasons explained in a later section it is necessary to measure the vapor flow characteristics in order to determine accurately the pressure drop across most porous plates. Through testing and analysis it was found that these flow tests must be run at true operating exit pressures because the flow is free molecule in nature and continuum flow does not apply. Through the use of these flow characteristics (Figure 3), the solid-vapor equilibrium data for water (Figure 2), and the heat transfer equations presented in a later section, theoretical performance has been correlated accurately with test data for the sublimation mechanism described here.

If the input heat flux is increased, the vapor pressure drop across the porous plate increases causing the sublimation temperature to rise accordingly. This results in a reduction in the ice layer thickness in order to satisfy the heat conduction requirements. Eventually the ice layer will disappear completely when the heat flux is sufficient to cause the vapor pressure at the inlet face of the porous plate to be greater than the triple point pressure. It is at this point that the evaporation mechanism begins to occur. However, if the pore size distribution is non-uniform, the heat flux at which this transition occurs will vary with location on the plate due to inequalities in vapor pressure drop, resulting in mixed mode operation.

5.2 Evaporation Mechanism

With the evaporation mechanism, the phase change occurs at pressure levels above the triple point. The absence of a solid ce layer to prevent liquid from passing through the porous plate requires that some other mechanism retain the liquid if supply pressure to ambient pressure differentials are to be greater than the vapor pressure drop. It was found that surface tension supplies the necessary restraining force for preventing liquid from passing through the porous plate. The head of liquid which a pore can retain by surface tension is inversely proportional to the equivalent radius of the restriction. Thus, in sintered metal powder plates, liquid enters the pores until the integrated restrictive force balances the pressure differential. If the pore size is too large to support the water feed pressure, breakthrough of liquid will occur when the input heat flux prevents operation in the sublimation mechanism. The surface of the meniscus formed by the liquid restrained in the porous plate is exposed to the lower pressure ambient allowing evaporation to satisfy the heat rejection requirement. Similar to the sublimation mechanism, the evaporation temperature is governed by the vapor pressure drop of the porous plate in conjunction with the liquid-vapor equilibrium pressure characteristic of the coolant.

Theoretically, if the porous plate were composed of straight through pores of constant cross section in a hydrophobic combination, analytical performance predictions could be made. With this idealistic porous structure the meniscus would restrain

5.2 Continued

the liquid at the pore inlets and the entire plate thickness would represent a known or measurable resistance to vapor flow. Under these conditions the vapor pressure at the phase change could be used to obtain the evaporation or sink temperature from vapor-liquid equilibrium data. Standard heat conduction across the liquid layer would then complete the analysis for performance. However, because the liquid is restrained at some undefinable depth in sintered powder plates, it is not possible to predict the vapor pressure, and, therefore, analytical performance predictions for this mechanism can be expected to be difficult and to require empirical data.

5.3 Mixed Mode

Increasing input heat flux will cause a direct transition from the sublimation mechanism to the evaporation mechanism if the pores are regular and uniform and sufficiently small for surface tension to prevent liquid breakthrough. However, porous plates suitable for fabricating full sized units contain a random distribution of pores with respect to both size and shape causing an operating region which has been called the mixed mode. The point of transition for any single pore is dependent on its equivalent radius and ultimately the vapor pressure drop produced by the pore. In the mixed mode of cooling, phase change occurs at local temperatures above and below the triple point depending on the local pore geometry. As a result of a distribution of pore sizes an averaging effect exists and if the plate is of reasonable thermal conductivity the effective plate temperature has been found to

5.3 Continued.

remain constant and very near the triple point for a wide range of heat fluxes. The cooling requirements of current space vehicle applications are at a level corresponding to this mixed mode, permitting design calculations to be based on a triple point sink temperature.

The mixed mode of cooling is unique in that a wide range of porous structures will exhibit the same heat rejection capability. The smaller pores are the first to undergo the transition from the sublimation to the evaporation cooling mechanism since they present the highest vapor pressure resistance. This is quite fortunate because these smaller pores are more capable of retaining liquid behind the porous plate by surface tension, while the larger ones remain plugged by ice. It is this order of events which allows operation in the mixed mode over a wide range of heat fluxes with liquid supply pressures higher than the water retention capability of the largest pore.

6.0

SELECTION OF POROUS PLATE

A wide variety of porous materials is available, and from thermal considerations, many of these may be practical. This study was primarily directed towards defining the pertinent thermal mechanism so that mission and manufacturing requirements can be evaluated in terms of their effect on performance. It is felt that the most valuable presentation on the selection of a porous plate is one that gives information in terms of the plate characteristics rather than one which attempts to talk in terms of specific mission requirements. Guides to the selection of porous plates will be discussed under two broad categories; Porous Structure and Material.

6.1

Porous Structure

The performance of the porous plate is primarily influenced by the holes, their number, dimensions and shape. Only regularly shaped holes are amenable to explicit analytical treatment. Few actual materials can approach the regularity desired for analytical treatment; these are generally of glass or plastic material and present fabricating and compatibility problems. At the inception of this investigation only sintered particle plates were available in materials considered immediately suitable for use in compact heat exchanger designs. These have distressingly irregular hole sizes and configurations. The experimental portion of this investigation was generally confined to tests of these plates where average properties were varied, to show if the analytical treatment of regular holes could be applied to the average hole characteristics of real plates.

6.1.1 Pore Geometry -- Three readily discernible categories appear. Pores of extremely uniform size and regular shape can be found in some glass filter materials. Very uniform but rather irregularly shaped pores can be found in impregnated fiberglass material. In the third category fall the non-uniform and irregular sized pores of the sintered particle metallic plates. This third category has received the bulk of the effort in this study. There is a continuing conflict between the convenient description of these plates and items of interest concerning thermal performance. Were it convenient to measure hole size, number, and distribution explicitly, it would be a far simpler task to express the performance of a plate.

When spherical particles are uniformly arranged, the hole size, shape, and number of holes can be explicitly defined. Also, the porosity is a function of the arrangement rather than the size of the particles. Figure 4 gives a visual illustration of some of the possible regular arrangements. Though sintered particle plates are formed from essentially spherical particles, the fabricating process of rolling sintering and particle size variation produces a plate whose properties can be defined only by measurement of gross parameters; such as flow, density, etc.

Before indicating what measurements are practical, it appears desirable to consider the hole characteristics that appear meaningful in the analytical treatment. First, open area is important; therefore, it is desirable to maximize the number of holes. Then the equivalent diameter of a hole is important as this influences the ability of surface tension forces to

6.1.1 Continued.

withstand a feed pressure. This puts an upper limit on the hole size. The third item of interest is the flow characteristics. The path length and cross section are the primary geometric factors of interest. In the modes of operation where flow is important it is desirable to minimize the pressure loss. The length must be minimized and the sectional area maximized. These characteristics point toward a fixed uniform hole size. However, the realities of porous plate construction require a balance to be achieved between increasing the number of pores and adjusting the diameter. In view of the strong dependence of the plate properties on the manufacturing process -- the features of which are of a proprietary nature -- it is very desirable at this stage in the development to concentrate on measurable characteristics of the porous plates.

Based on the theories developed in this study, it should be possible to establish upper and lower limits on the vapor flow characteristics of the porous plates to be used for a particular cooling application. These limits can then serve as a specification along with the water retention pressure when manufacturing porous plate water boilers. The upper flow limit is established by the pore size dictated by water retention requirements and the plate porosity or void fraction. The heat rejection requirements establish the lower flow limit and the pressure drop across the porous plate for both flow limits.

Hole size is a more difficult quantity to obtain. Observing the surface under suitable magnification shows only void space at one level which is inherently different from the inner

6.1.1 Continued

layers. No direct measurements of hole size are possible. However, the maximum size hole and an estimate of its size can be conveniently made by running a bubble point test, which is explained in Appendix D. In addition, a qualitative distribution of the holes is apparent. Uncertainty in the distribution of the various hole sizes still presents a problem in uniquely specifying sintered particle porous plate with bench type qualification tests.

6.2 Material

Several material properties influence the selection of material for porous plates, including, but not necessarily restricted to, thermal conductivity, corrosion, wettability, strength, vacuum stability, and fabrication compatibility. The first three were given explicit attention in this study. The others are of lesser importance, but still significant, as we found in our attempts to form the transport fluid modules of Phase IV.

6.2.1 Thermal Conductivity -- Conduction is the prime mechanism by which heat is transferred to the sublimating evaporating interface. In the sublimating mode the analysis places the interface at the interior surface of the porous plate, and in this case thermal conductivity of the plate should have little effect. It can be postulated that the interface is at some undefined plane inside the plate in the mixed and the evaporative modes of operation, and that in these cases heat conduction within the plate should be important. Metallic porous plates, varying in

6.2.1 Continued

thermal conductivity over a 25-1 range, were tested, and the results confirmed our first hypothesis that in the sublimation mode plate conductivity was unimportant. However, the results of these tests implied that this is also true for the mixed mode. The evaporative mode was beyond the range of our test set-up.

6.2.2 Corrosion Resistance -- The corrosion problem was investigated

with respect to nickel porous plates since these plates were currently being used in development units for proposed space exploration vehicles. It was found that when a nickel porous plate is exposed to water a non-sealing layer of nickel hydroxide continues to form on all exposed plate surfaces. It was additionally found that if the nickel plates have prior oxide build-up, exposure to water will result in the formation of some hydrated nickel oxide as well as the nickel hydroxide. A substantial volume increase occurs with time in the surface film as a result of these reactions, closing a large number of the smaller pores and eventually reducing the heat rejection capability of the device.*

In the investigation where this problem was identified, three potential causes of degradation were examined by exposing three identical nickel porous plates to test water in three different ways, in an effort to isolate the cause of deterioration.

One plate was run continuously for 100 hours, exposed

* The specific gravity of nickel compared to the various forms of corrosion is a measure of the volume change. The specific gravities are:

$Ni = 8.90$	$Ni(OH) = 4.1$
$NiO = 7.45$	$NiOH_2 \cdot O = 4.1$

6.2.2 Continued

to the normal operating conditions and presumably to all potential causes of degradation. A second plate was force flushed with the equivalent amount of water to show if entrained organic or inorganic solids caused the degradation. A third plate was soaked for the same period without evaporation to show if bacteria growth or reaction with water causes degradation; these alternatives could be identified by subsequent analysis of the plate.

Performance checks and porous plate characteristics measurements were made on these plates before and after exposure, and the results are presented in Tables 1 and 2. It was concluded from these results that degradation of performance became significant after about 200-300 hours of exposure to water and is a result of corrosion which caused plugging of the pores. The other potential causes -- solid particle retention and salt deposition -- might be important under different conditions such as longer time duration and higher initial concentrations.

Several approaches exist for meeting such problems. The selection must be made in consideration of the mission requirements. The most obvious is selection of an alternate material which is more passive to water. In some cases the degradation can be accommodated by design. Inhibitors in the water and the use of other fluids are also possible.

6.2.3 Wettability -- The analyses conducted in this study show that, in the evaporative mode and under starting transients, the

6.2.3 Continued

wettability of the plate may have significant effects. A non-wettable plate would have poor performance in the evaporative mode because the heat sink temperature would increase rapidly with heat flux. On the other hand, a non-wetting plate would exhibit some advantage in improved water retention capabilities. In theory either a wetting or non-wetting plate should restrain a static head, the difference being the face at which the fluid is restrained. Fluid restrained at the upstream face of a non-wetting plate would tend to be stable with respect to transients in the water supply pressure. Fluid restrained at the outer face, as for a wettable plate, would be expected to bridge the holes under a water supply pressure transient, causing a breakdown of the entire restraining mechanism. These hypotheses were not examined experimentally.

6.2.4 Other Material Considerations -- The remaining material considerations -- strength, vacuum stability, and fabrication -- were not an issue in this study, but a brief comment on the observations with respect to these matters may be informative.

The sintered plates do not have high strength characteristics. When testing and handling unsupported plates it appeared possible to fracture a plate rather easily. This fracture would become apparent in an operating plate as an ice filament extending from the outer face of the plate. Apparently the bond between particles would be broken, effectively increasing the pore size.

6.2.4 Continued.

Fabrication technique is a field in itself. Both material and configuration factors are important. Brazed modules of a standard type, where the porous plates were continuously supported by fins, were made without difficulty. However, where unsupported plates were specifically required for experimental purposes, a great deal of difficulty was encountered. To solve this problem and get on with the experimental program a non-metallic bond was used, although this approach would probably not be considered acceptable for production articles.

Vacuum stability is not a problem with metallic plates, but early in the study some plastic materials were eliminated for this reason.

7.0 MATHEMATICAL MODELS

Three modes of operation have been indicated, each requiring a slightly different form of analysis. The three modes are discussed in the following sections; an additional section presents a treatment of the flow losses through a plate discharging to vacuum ambients.

7.1 Sublimation Mechanism

This mechanism or mode of operation represents the condition when an ice layer exists on the liquid reservoir side of the porous plates. Operating a unit with colored water conclusively showed that this ice layer prevents liquid from entering the porous plate. In addition it demonstrated that the individual particles of ice actually move toward the porous plate with time while the ice layer maintains a constant thickness. In order to satisfy these observations and the input heat flux requirement the ice layer must sublimate at the porous plate face at the same rate that ice is formed at the ice liquid interface.

An analysis of the sublimation mechanism including energy transfer by conduction and convection is presented in Appendix L. This analysis shows that the temperature distributions across the liquid and ice layers are essentially linear for the range of conditions for which this device will be employed. Suitable results can thus be obtained by considering energy transfer by conduction alone. Referring to Figure 5, the heat transfer across the liquid and ice layers can be expressed as

$$q_1/A = q_0/A = (k_L/L)(T_0 - 32) \text{ and } q_2/A = (k_I/I)(32 - T_g)$$

where k is the effective thermal conductivity of the respective layers. The boundary conditions of the ice layer are:

$$q_2/A = q_1/A + \omega/A \cdot h_f$$

7.1 Continued.

at the liquid interface, and

$$q_2/A = \omega/A \cdot h_s$$

at the sublimating face, where h_f and h_s are the heats of fusion and sublimation, respectively.

By combining these expressions algebraically, the temperature of the heated surface can be written as:

$$T_0 = 32 + \frac{1}{k_1} \left[q_0/A \cdot S - k_1 \left(1 - \frac{h_f}{h_s} \right) \cdot (32 - T_s) \right]$$

where T_s is the sublimation temperature and is related to the local pressure for solid-vapor equilibrium.

The ice layer thickness, which was one of the measured quantities when testing porous plates under this mode of operation, can also be derived from the above expressions, giving

$$I = \frac{k_1(32 - T_s) \cdot (h_s - h_f)}{q_0/A \cdot h_s}$$

7.2 Evaporation Mechanism

Tests run with the ambient pressure above the triple point pressure precluded the existence of ice in any area of the porous plate. Under these conditions the only obvious assumption is that the liquid is retained behind the porous plate solely by surface tension and the input heat flux requirement is met by evaporation. The liquid head retained by surface tension was found to be identical to the liquid breakthrough pressure, as determined independently for the porous plate operated in

7.2 Continued.

this mode, proving these postulates. When exhausting to a low ambient pressure less than the triple point pressure, as normally intended, a porous plate will operate solely with this evaporation mechanism if the heat flux is sufficient to maintain the interface vapor pressure above the triple point.

Assuming a pore is small enough to support a liquid head by surface tension the wettability of the porous material determines where the liquid is restrained. In the case of a hydrophobic material the liquid would be restrained at the upstream end of the pore; a hydrophilic material would restrain the liquid at the downstream end of the pore. Clean metals and glass are generally completely wetted by clean liquids, but it is frequently found that these materials tend to be hydrophobic if the liquid or surface becomes even slightly contaminated.

For this mode it was necessary to assume that the liquid was restrained at the downstream end of the pores, as by a hydrophilic material, in order to correlate the test results. By assuming that the liquid is at the downstream end of the pores it is not necessary to account for a pressure loss from the evaporating surfaces to the ambient. This is only approximate because a pressure gradient exists above any evaporating surface but it is usually negligible. Since the input heat flux is simply the heat conducted across the liquid layer and the porous plate, the temperature of the heated plate can be expressed as:

7.2 Continued.

$$T_o = T_e + q_o/A \cdot 1/U$$

where T_e is the evaporation temperature corresponding to the ambient pressure and U is the equivalent thermal conductance.

The equivalent thermal conductance is then given as

$$1/U = \delta/k_l + t/k_p$$

where k_l and k_p are the equivalent thermal conductivities of the liquid layer and porous plate, respectively. For these tests natural convection was eliminated and no fins were included so k_l is the conductivity of water, and k_p can be expressed as

$$k_p \approx k_l P + k_m(1 - P)$$

where P is the porosity of the plate and k_l and k_m are the thermal conductivities of water and the porous plate metal respectively.

7.3 Mixed Mode

The existence of the mixed mode is possible because sintered metal porous plates have non-uniform pores. This non-uniformity is not quantitatively definable, which makes exact theoretical treatment of this mode impossible. However, this does not represent a critical situation because performance can be predicted, with a reasonable degree of accuracy, by making a simple assumption.

7.3 Continued

The porous plate temperature can be assumed to be at the freezing point of the fluid. Then heat source temperatures may be calculated with knowledge of the conduction path between the porous plate and heating surface. The assumption of porous plate temperature is intuitive if one realizes that all large holes will have some ice, i.e., a temperature slightly less than freezing, and the temperature of the smaller holes will be slightly above. The range of this mode corresponds with moderate heat fluxes, so that it seems unlikely that the smaller pore temperatures would tend to get very high. Furthermore, if plates of high conductivity are used, it will be necessary for the plate to be at 32°F for the larger pores to be blocked. This was confirmed by temperature measurements on the surface of porous plates when operating in the mixed mode.

Some theoretical numbers can be made which further support this mode and place an upper bound on its range. By use of the water retention tests (see Appendix D) a maximum hole size can be estimated. With this hole size a heat flux that will raise the pressure above the triple point can be calculated. This is the obvious upper bound for this range.

The heat flux can be assumed to be proportional to the area of the hole. The pressure loss, which is shown in the next section to be characteristic of free molecule flow, is inversely proportional to the radius cubed. It can be immediately concluded that for holes smaller than the maximum there exists a lower heat flux at which the pressure loss in these holes will be large enough to raise the interface-pressure above the triple point, hence the mixed mode.

7.4 Free Molecule Flow Through Porous Media

In order to determine the vapor pressure at which the sublimation or evaporation phase change occurs the porous plate flow characteristics must be defined. The phase change temperature can then be obtained from equilibrium vapor pressure data for the particular substance and phase change process.

Gas rarefaction must be considered because of the very low ambient pressure to which the porous plates are exposed. In considering this effect, the molecular mean free path, λ , is commonly used to identify the flow regime. If the mean free path is small compared with the most significant dimension of the system, gas flow can be treated as continua, and macroscopic properties such as density, velocity, and temperature may be assumed to vary continuously in time and space. Rates of transfer of momentum and energy in continuum flow are governed by a series of random molecular collisions, allowing rapid adjustment of the gas state in the event of flow disturbances such as friction or heat transfer. When the gas is rarefied so that the mean free path is not negligible compared to the most significant dimension, intermolecular collisions become less frequent and molecules which do not strike the boundaries of the system are unable to come into equilibrium with the boundaries.

Depending on the degree of gas rarefaction, gas dynamics is commonly sub-divided into three flow regimes: continuum flow, slip flow, and free molecule flow. Continuum flow exists when the mean molecular free path λ is small compared to the most

7.4 Continued

significant dimension of the flow system L , whereas free molecule flow occurs when λ is large relative to L . The slip flow regime exists when λ and L are of the same order of magnitude.

In the case of flow in porous media the most significant dimension is the equivalent pore diameter. In this study the equivalent pore diameter of the porous plates tested varied from 0.5 to 15 microns with most of the pores approximately 1 - 2 microns in diameter. From modified kinetic theory the mean molecular free path can be computed from the equation

$$\lambda = \frac{\mu}{p} \cdot \frac{RT}{2 \epsilon_0}$$

where μ is the gas viscosity, R is the gas constant, and p and T are the pressure and temperature respectively. At the triple point pressure and temperature the mean molecular free path for water vapor is 6.95 microns, indicating that free molecule flow exists at this pressure or any lower pressure as occurs in the sublimation mechanism. At slightly higher pressure levels, which will occur in the evaporation mechanism, flow characteristics may tend toward the slip flow regime.

Free molecule flow through long narrow tubes can be expressed as

$$\omega = \frac{8}{3} \sqrt{\frac{2 \epsilon_0}{\pi RT}} \cdot \frac{P_1 - P_2}{R} *$$

where

$$R = \int_0^L \frac{C}{A^2} dx$$

* J. K. Roberts, and A. R. Miller, "Heat and Thermodynamics," 5th Edition, Interscience Publishers, Inc., New York, 1960.

7.1 Continued.

- W = gas flow rate
- R = gas constant
- P_1 = inlet pressure
- P_2 = outlet pressure
- T = absolute temperature
- g_0 = gravitational constant
- R_f = flow resistance
- l = flow length
- C = tube circumference
- A = tube area

The non-uniform pore size distribution and unknown variation in circumference and area with flow length prevent evaluating the flow resistance, R_f , to free molecule flow through porous plates. However, the equation does show the nature of free molecule flow and how it can be correlated with experimental results for porous plates. Since the flow resistance is a function only of geometry, experimental data can be used to determine the equivalent resistance to flow through porous plates. Also, it is apparent from the flow equation that the flow rate is proportional to the pressure differential, but not the absolute pressure as is the case for continuum flow. Using these established effects, experimental data for free molecule flow through porous plates can be correlated in the simple form

$$W/A = K\Delta p$$

8.0

DISCUSSION OF TEST RESULTS

Several experimentally demonstrable points are revealed by the analysis. The most obvious point is the existence of the modes. The flow regime can also be demonstrated by experiment. A third area of effort in the experimental program involved the demonstration of the effects of various plate characteristics on heat rejection performance. A final phase involved the testing of transport fluid heated modules. This effort has not been reported on previously and is treated in more detail in a separate section.

8.1

Performance Modes

The analysis postulated a mode of operation -- appropriately named the sublimation mode -- which exhibited an ice layer. The test module had plexiglass sides so that it was possible to observe the behavior of this ice layer. For a particular plate the analysis shows the thickness of the ice layer to be dependent on the heat flux. For different plates at a constant heat flux the ice thickness depends on the gas pressure drop across a plate discharging to a vacuum. Ice layer thickness and heater plate temperature versus heat flux for a particular plate is illustrated in Figure 6. The solid curves; calculated by the theory of section 7.1, show that a satisfactory correlation exists. The heat flux at zero ice layer thickness represents the upper bound of the sublimation mode. The measured flow characteristics used in predicting the performance of this plate are presented in Figure 7 along with the flow character-

8.1 Continued

istics of other plates used in the program.

Proof of the existence of the evaporation mode in exactly the same context as was presented in the analysis is difficult to achieve because of the high heat fluxes required. These are higher than those which were normally encountered in our current applications, and our test units could not safely provide them at low ambient pressure. However, the essential aspects of the evaporative mode are exhibited if we merely exclude the possibility of the existence of ice. This was done by raising the ambient pressure to a level slightly above the triple point. The performance of a plate operated in this fashion is shown in Figure 8. The solid line represents the predicted results. The attention given this mode has been restricted by the experimental limitations and by a lack of immediate interest in higher sink temperatures. Items of interest in the evaporation mode involve the effects of wettability on performance and water retention and the change in flow regimes at higher mass fluxes and pressure levels. These might be the objective of additional experimentation.

The third mode, the mixed mode, results from a distribution of the hole sizes as explained in a previous section. Each hole, by the theory presented, will go directly from the sublimation to the evaporation mode. The local heat flux at which this occurs is dependent on the radius of the hole. Therefore as

8.1 Continued.

the heat flux is increased in a given plate there is a period of operation in which part of the holes have undergone the transition and others have not. For this mode performance correlation is achieved by assuming a constant sink temperature which is the triple point of the fluid. A comparison of the measured and predicted heat rejection performance of a plate operating in the mixed mode is presented in Figure 9, illustrating adequate correlation.

The heat fluxes occurring in the mixed mode and the upper range of the sublimation mode are those which are normally encountered in fluid cooling applications. In the remaining experimental work the effort was directed toward identifying the effects of changing plate characteristics when operating in these modes.

8.2 Effects of Plate Characteristics

The plate variables selected for investigation were thickness, density, particle size, and plate conductivity, because these are quantities which can be specified in the plate manufacture, and it is possible to vary them independently. For each variable a range was selected which might prove suitable for porous plate usage. Three plates, which spanned this range, were selected for each point investigated. In addition, four plates were ordered to an identical specification so that reproducibility could be checked.

8.2 Continued

It is important to recall that the theory presented requires that the performance of a plate be dependent on the pressure loss in the sublimation and evaporation modes. An examination of the pressure loss data illustrates the variations that might be expected from these plates. A concise statement of the results of this phase of the testing will aid in the presentation. No significant variation in performance could be attributed to the controlled variables over the range considered in this study. First, it is important to examine the control plates, those ordered to identical specifications. The results of the performance tests are shown in Figure 10. A 7°F band bounds the data, and at any heat flux a consistent order among the plates does not exist. A check of the flow data for these plates shows that there is indeed a difference but it is very orderly. Therefore little use can be made of this data to predict or explain the spread in performance. One point can be made. The lack of dependence on flow indicates these plates operate in the mixed mode. Without exhaustively going through the details of each variable, the above mentioned conclusion can be illustrated by observing Figure 11, where all performance data is presented on a single plot. The boundaries of the points are hardly increased over the control set. It is therefore concluded that the range of variables (density, thickness, pore size, and plate conductivity) considered in this program has little importance in determining the performance when operating in the mixed mode. Despite the

8.2 Continued.

data spread, an approximate performance prediction is given by the assumption of a triple point sink temperature with the resistance to heat dissipation being provided by the conduction path.

Our theory offers additional potential in resolving the existing spread in performance in the mixed mode. The importance of pore radius, or more precisely pore shape, on the transition heat flux between the principal modes has been stated. It is conceivable that a detailed knowledge of the pore size distribution would allow a prediction of performance in the transition region. Such a detailed description of a porous plate is beyond the scope of this program.

Despite the lack of a precise analytical method of prediction in this mode, it represents the most practical operating range for current applications. The heat sink temperature is adequate and the heat fluxes are maximized providing the minimum size unit.

9.0 Configurations for Transport Fluid Cooling

The heat rejection performance of the porous plate boiler was investigated experimentally and theoretically for electrically heated modules in which the plates were in an as-received condition. One of the current uses of this device is the cooling of a transport fluid in a compact heat exchanger such as the one shown in Figure 1. This unit incorporates fins which are brazed on the transport fluid and water sides for improved thermal performance and structural rigidity. The manufacturing process to which the porous plates are exposed during fabrication of this type of unit introduces a variety of practical considerations which were investigated in the final phase of this program.

The brazing of a heat transfer fin in the water passage is easily accounted for in the theoretical analysis by adding the conductance of the fin in parallel with the water. However, the brazing process can be postulated to disturb or change the original porous plate properties by blocking pores or disturbing the original bonds between sintered particles. An additional problem may be introduced by the fins because the heat flux at the transport fluid inlet may be sufficiently high to cause liquid breakthrough due to the elimination of ice plugs in pores which are too large to restrain the liquid by surface tension.

With these questions in mind four different glycol heated test modules were designed (Drawing No. 134X-52 to 55) to evaluate the existence of such problems and to illustrate potential solutions. The porous plates selected for these modules and their performance in an

electrically heated module prior to manufacturing are listed in Table 5. These plates were ordered to identical specifications but it is apparent that for the same heat flux there is a difference of several degrees in heater plate temperature. The glycol circuits of all four units were intentionally made the same so that water side effects could be isolated. A photograph of one of the glycol heated modules is shown in Figure 12.

Module 136X-54 is of conventional construction with nickel fins brazed to both the porous plate and the fluid parting sheet. This unit was used to demonstrate the differences from an electrically heated clean porous plate due to a manufacturing process. This unit was also used to evaluate breakthrough limits over a wide range of heat fluxes and glycol inlet temperatures which exceeded current applications by a considerable magnitude.

Module 136X-55 was similar to the previous one but incorporated a variation in the water side heat transfer conductance; increasing in the direction of decreasing glycol temperature. This change was intended to provide a more uniform heat flux at the porous plate to retard liquid breakthrough if the problem existed with the previous unit. Some sacrifice in heat rejection capability is obvious with a unit of this type but it may be necessary for high temperature applications.

The third module, 136X-53, was intended to eliminate blocking of pores by using fins which are shorter than the water passage gap and were not brazed to the porous plate. Another intention was the possibility

of controlling breakthrough due to high heat flux by this alternate fin arrangement.

The fourth module, 136X-52, did not have any fins in the water passage; similar to the electrically heated modules, and was intended as a reference unit for the other three modules. It served to show the combined effects of adding fins to the water passage; aside from what theory would indicate, and the brazing of fins to the porous plate.

Some of the design anomalies requested in these glycol modules - the unsupported porous plate, fin variations, and small size - caused manufacturing difficulties. Problems in attaching the porous plate to the two modules where fins do not support the plate were finally solved by using an adhesive in place of the originally intended braze bond. The only change that this introduced was to keep the porous plate from being exposed to a heating cycle which actually serves to preserve the originally intended reference level. The conventional module was fabricated with a minimum of effort. Based on these experiences an extensive fabrication development program will be necessary if performance criteria for some future mission requires similar unconventional designs. However, the results of the performance tests, discussed below, showed that the conventional design was most effective for current space vehicle transport fluid cooling requirements.

Predicted performance calculations for the conventional module (136X-54) were made based on the theory presented in section 7.3; the details

of which appear in Appendix A. An effectiveness plot; effectiveness vs mass flow, given in Figure 15 was shown to be independent of glycol inlet temperature within the temperature range (60°F to 120°F) used in the test program. The performance calculations obviously do not reflect such considerations as pore blockage and thus they can be used as another reference for evaluating the effects of manufacturing on the porous plates. Also shown in Figure 15 is the measured performance of this conventional module. The actual performance was always less than the predicted, but the superior performing runs were close to the predicted curve. Figure 15 also shows an apparently significant spread in the data which is influenced by glycol inlet temperature. This is contrary to the predicted performance calculations in Appendix A which shows the inlet temperature dependence to be negligible. Comparing the test data for the conventional module with that for the other modules in Figures 13, 14, and 16 it is apparent that some other parameter besides inlet temperature is influencing the spread in the test data. If temperature level were producing this spread it would be expected that a consistent order would exist, but no such pattern exists.

One possible explanation for the data spread is performance deterioration with time. However, the sequence in which the tests were conducted on each module and the order of the performance levels in terms of inlet glycol temperature given in Table 3 shows no obvious reason for expecting the data spread to be caused by deterioration in performance. Another potential explanation for the data spread is maldistribution of the glycol flow since independent studies at

Hamilton Standard have shown erratic distribution can produce similar effects on performance for comparable levels of mass velocity. The small size of these modules and the presence of vapor pockets in a unit tends to accentuate the effects of maldistribution. The glycol heated modules were intentionally designed with four one inch wide glycol passes to avoid maldistribution but possibly the problem was not entirely eliminated.

The procedure taken in setting up the various test conditions was also analyzed in light of the spread in test results. The temperature level was established and then the procedure was to vary the glycol flow rate over the desired range keeping a constant inlet temperature. When the temperature was changed the flow to the module was usually shut-off until the new level was established. This procedure could lead to the illusion of an inlet temperature dependence whereas the more logical explanation is a glycol flow distribution which was different for each inlet temperature. To further check this theory attributing the data spread to erratic glycol flow distribution; module 136X-55 was run twice at the same temperature level of 90°F on different days. This data, shown in Figure 16, further supports the conclusion that the data spread is due to a changing glycol flow pattern and not glycol inlet temperature. The only obvious explanation for the data spread is a change in glycol flow pattern.

The relative performance of the various glycol heated modules is illustrated in Table 4 in terms of mean values of effectiveness at various flow rates. The performance follows the anticipated pattern with the conventional unit being superior to the others. The unit

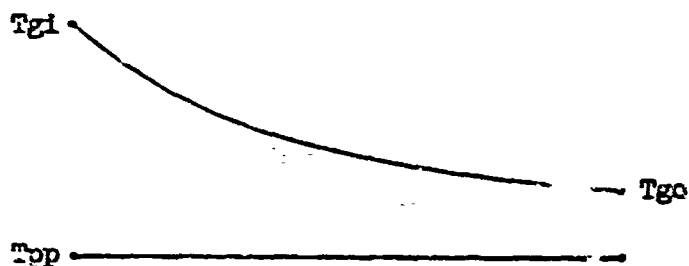
incorporating a variation in water side conductance exhibited the second best performance while the one without fins and the one with short fins not brazed to the porous plate are very close but of inferior performance. Apparently blocking of some of the pores by brazing fins to the porous plate is not sufficiently detrimental to overcome the advantage of the improved heat conduction of the fins. However, if the predicted performance is assumed as a reference level the theoretical advantages of brazing the fins to the porous plate were not completely realized. Several things could explain this deficiency - blocking of some pores, poor brazing at the ends of the fins, or as discussed above; glycol maldistribution.

To evaluate liquid breakthrough limits the conventional module, 136X-54, was started up at increasingly higher glycol inlet temperatures with a water supply pressure of 10 psia. The procedure for a start-up test was to establish the test chamber vacuum, glycol inlet temperature, and water supply pressure; then once the unit was hot soaked at the glycol temperature and all residual water evaporated; the water supply valve was rapidly opened. The test module was successfully started in this manner without inducing breakthrough for hot soaked glycol temperatures as high as 150°F, which is the upper limit of the test rig. These results indicate that a conventional transport cooling porous plate boiler can be made with suitable hot start-up characteristics for proposed space vehicle applications. It is thus not necessary to resort to adjusting the water side heat transfer paths; which reduces performance, so as to retard liquid breakthrough.

APPENDIX ASAMPLE CALCULATIONS FOR THE
GLYCOL HEATED MODULE #136X-54

This module used a sintered porous plate for which operation solely in the evaporation mode is unlikely. The sublimation mode occurs at the low heat flux range and is of only modest interest. The performance prediction is detailed for the mixed mode. For the mixed mode reference to section 4.3 shows that the sink temperature is constant at the fluid triple point. For the case considered here, the sink temperature is 32°F.

The temperature profile for this heat exchanger is:



The effectiveness of the heat exchanger is defined as:

$$\epsilon = \frac{\Delta T_{\text{actual}}}{\Delta T_{\text{max}}} = \frac{T_{gi} - T_{go}}{T_{gi} - T_{pp}}$$

This can be written in terms of the fluid properties and the geometry of the unit.

$$q = UA \Delta T_{LM} = W_g C_g (T_{gi} - T_{go})$$

where

$$\Delta T_{LM} = \frac{(T_{gi} - T_{pp}) - (T_{go} - T_{pp})}{\ln \left(\frac{T_{gi} - T_{pp}}{T_{go} - T_{pp}} \right)}$$

and

$$\frac{T_{gi} - T_{pp}}{T_{go} - T_{pp}} = e^{\frac{UA}{W_g C_g}}$$

$$\frac{T_{gi} - T_{pp}}{T_{gi} - T_{pp}} - \frac{T_{go} - T_{pp}}{T_{gi} - T_{pp}} = 1 - e^{-\frac{UA}{W_g C_g}}$$

$$\epsilon = \frac{T_{gi} - T_{go}}{T_{gi} - T_{pp}} = 1 - e^{-\frac{UA}{W_g C_g}}$$

It is only necessary to calculate UA for the particular unit.

$$UA = \frac{h_{eg} A_g \times h_{ew} A_w}{h_{eg} A_g + h_{ew} A_w}$$

where

h_{eg} = effective glycol film coefficient

h_{ew} = effective water side resistance

A_g = glycol side surface area

A_w = water side area

Evaluation of glycol side conductance.

Fin characteristics:

0.100" Ferr - 18 FPI - .002" tk

Stainless Steel

Pass width 1"

Pass length 4"

Number of passes - 4

Glycol fin area:

$$A_{fg} = \frac{W \cdot \text{FPI} \times \text{tk} \cdot (H - \text{tk})}{144}$$

$$= \frac{1(1-18 \times .002)(0.100 - .002)}{144} = 6.61 \times 10^{-4} \text{ ft}^2$$

Characteristic length:

$$D_{hg} = \frac{2(H-tk) \left(\frac{1}{FPI} - tk \right)}{H + \frac{1}{FPI} - 2tk}$$

$$= \frac{2(.0988)(.0556 - .002)}{0.100 + 0.0556 + 0.004} = 0.0686 \text{ in.}$$

The maximum Reynolds number is at the maximum flow rate and temperature.

Maximum Flow: 115 lb/hr

Maximum Temperature: 120°F

$$Re = \frac{Gg D_{hg}}{\mu}$$

$$= \frac{115}{6.61 \times 10^{-4}} \cdot \frac{0.0686}{12} \cdot \frac{1}{5.15} = 193.5$$

At such low Reynolds number fully developed laminar flow is assumed. Under these conditions the Nusselt number $\left(\frac{hg D_{hg}}{kg} \right)$ has been found to be a constant 3.65, for the conditions encountered.

$$Nu)_g = \frac{hg D_{hg}}{kg} = 3.65$$

There is a slight variation of kg with temperature.

$$kg = 0.224 \text{ Btu/hr-ft}^2\text{-}^\circ\text{F at } 60^\circ\text{F}$$

and

$$kg = 0.219 \text{ at } 120^\circ\text{F}$$

Solving Nu for hg it is found that

$$hg = 143.0 \text{ at } 60^\circ\text{F}$$

$$140 \text{ at } 120^\circ\text{F}$$

The temperature dependence is ignored in further calculations and hg is assumed constant at 140 Btu/hr-ft²-°F

$$h_e = 10 \text{ h}$$

where

$$\lambda_o = 1 - \frac{Ass}{A_{ts}} (1 - \lambda_f)$$

$$\lambda_f = \frac{\text{Tanh } U_f}{U_f}$$

$$\frac{Ass}{A_{ts}} = \frac{(H - tk) FPI}{(H - tk) FPI + (1 - FPI \times tk)}$$

$$U_f = \frac{2H}{2k} \sqrt{\frac{24 h}{k_f tk}}$$

$$\frac{Ass}{A_{ts}} = \frac{0.0988 \times 18}{0.0988 \times 18 + 0.964} = 0.655$$

$$U_f = \frac{0.100}{12} \sqrt{\frac{24 \times 140}{9 \times 0.002}} = 3.60$$

$$\lambda_f = \frac{\text{Tanh}(3.60)}{3.60} = 0.277$$

$$\lambda_o = 1 - 0.655 (1 - 0.277) = 0.527$$

$$\text{neg} = 140 \times 0.527 = 73.9 \text{ Btu/hr-ft}^2\text{-}^\circ\text{F}$$

$$\begin{aligned} Ag &= A_{ts} = \frac{WL}{72} \left[1 - (FPI \times tk) + FPI (H - tk) \right] \times N \\ &= \frac{1 \times 16}{72} \left[1 - (18 \times .002) + 18(3.1 - .002) \right] \times 1 \\ &= 0.609 \text{ ft}^2 \end{aligned}$$

$$\text{The Glycol Side Conductance } \text{negAg} \text{ is } 45.0 \text{ Btu/hr-}^\circ\text{F}$$

Water Side Conductance:

The water side is viewed as a conduction resistance only. The water feed rate is so low that there is no effect when considering the thermal performance.

$$h_{ew} = \frac{k_w}{H} \frac{A_w - A_f}{A_w} + \frac{k_f}{H} \frac{A_f}{A_w}$$

$$h_{ew} A_w = \frac{1}{H} [k_w (A_w - A_f) + k_f A_f]$$

The water side fins are

0.075" H 12 FPI .004" tk

Perforated nickel

98 hole/in² ±5

0.050 ±5 hole diameter

The water side fins are perforated to allow for water distribution. This perforation accounts for a significant area of the fin and must be included in the calculation of A_f .

Perforation Reduction Factor:

$$F_p = 1 - \frac{98(.050)^2 \pi}{4} = .808$$

$$A_f = WL (FPI) tk \times F_p$$

$$= \frac{4 \times 4 \times 12 \times 0.004 \times .808}{144} = 4.31 \times 10^{-3} \text{ ft}^2$$

$$A_w = \frac{4 \times 4}{144} = 0.110 \text{ ft}^2$$

$$k_w = 0.338 \text{ Btu/hr ft} \cdot ^\circ\text{F}$$

$$k_f = 35 \text{ Btu/hr ft} \cdot ^\circ\text{F}$$

$$h_{ew} A_w = \frac{1}{6.25 \times 10^{-3}} [0.338 (0.1057) + 35 (4.31 \times 10^{-3})]$$

<p>The Water Side Conductance $h_{ew} A_w$ 29.5 Btu/hr - °F</p>
--

$$UA = \frac{15.0 \times 29.5}{15.0 + 29.5} = 17.8 \frac{\text{Btu}}{\text{hr}^\circ\text{F}}$$

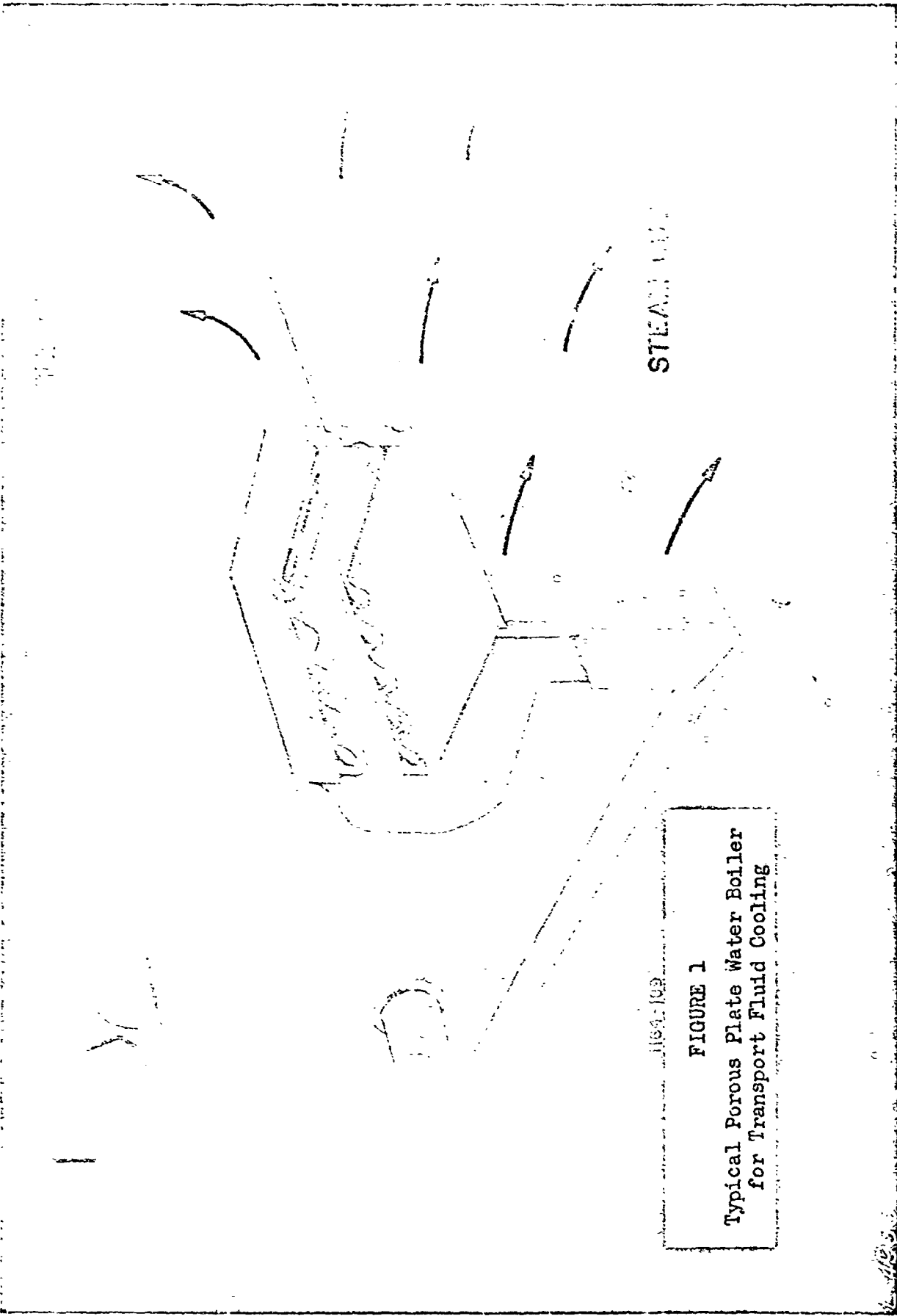
$$\epsilon = 1 - e^{-\frac{UA}{W_g C_g}}$$

$$C_g = 0.765 \text{ Btu/lb-}^\circ\text{F at } 120^\circ\text{F}$$

<u>W_g lb/Hr</u>	<u>UA/W_gC_g</u>	<u>$e^{-\frac{UA}{W_g C_g}}$</u>	<u>ε</u>
20	1.19	.303	.697
50	.475	.625	.375
70	.340	.710	.290
90	.264	.767	.233
110	.216	.808	.192

APPENDIX B

ILLUSTRATIONS



1154-109

FIGURE 1
Typical Porous Plate Water Boiler
for Transport Fluid Cooling

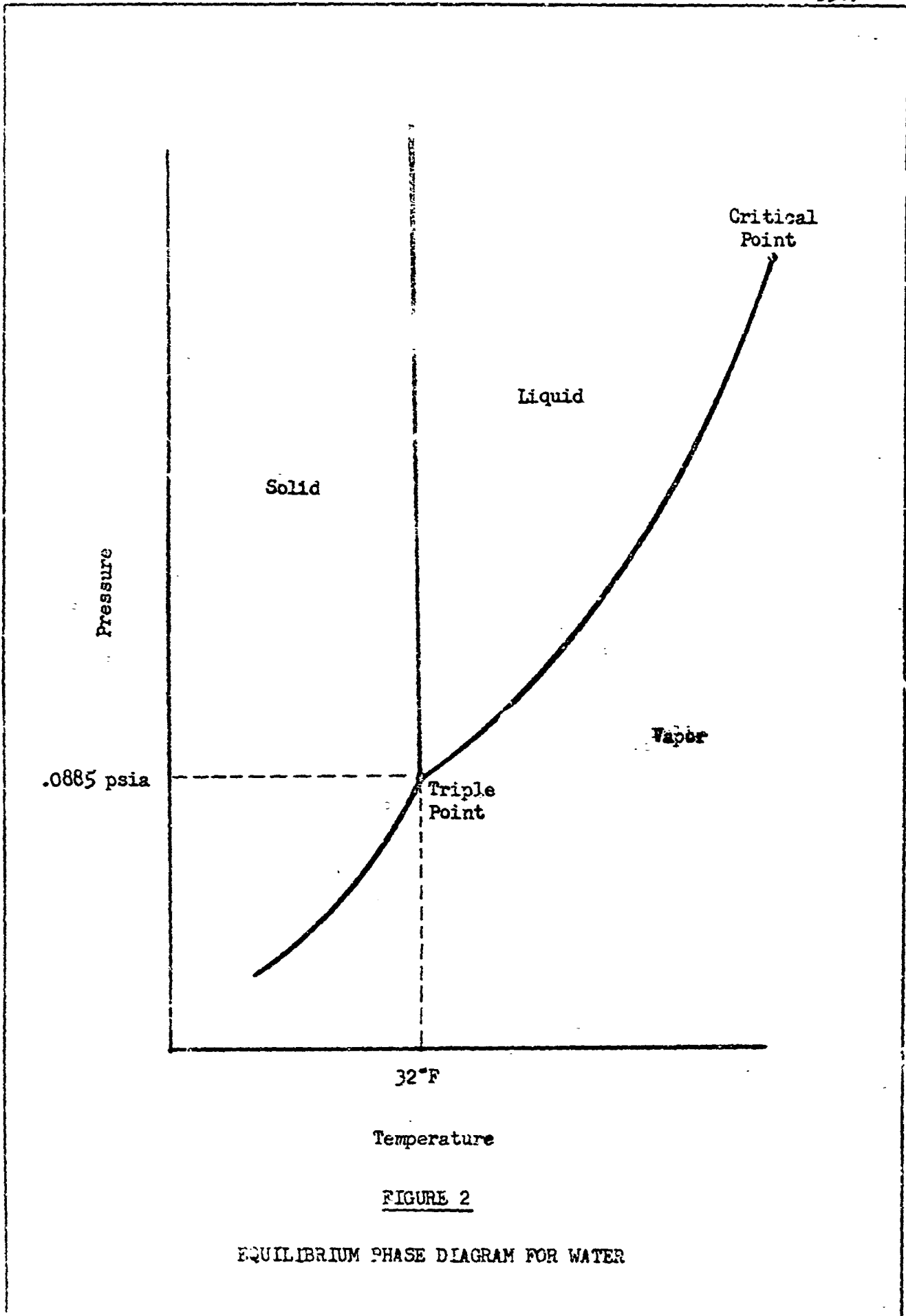


FIGURE 2

EQUILIBRIUM PHASE DIAGRAM FOR WATER

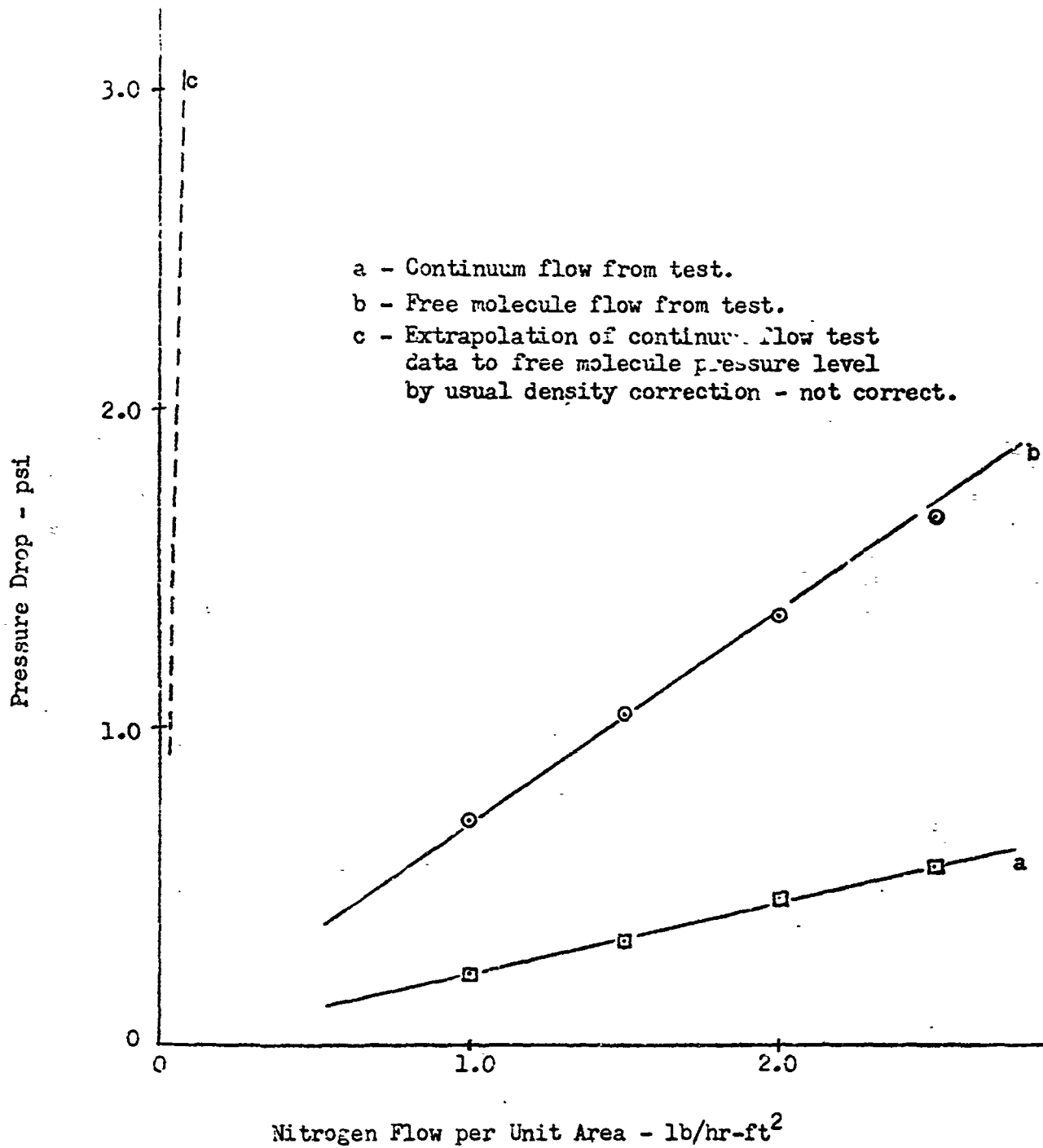


FIGURE 3

COMPARISON OF CONTINUUM FLOW AND FREE MOLECULE FLOW FOR PLATE C

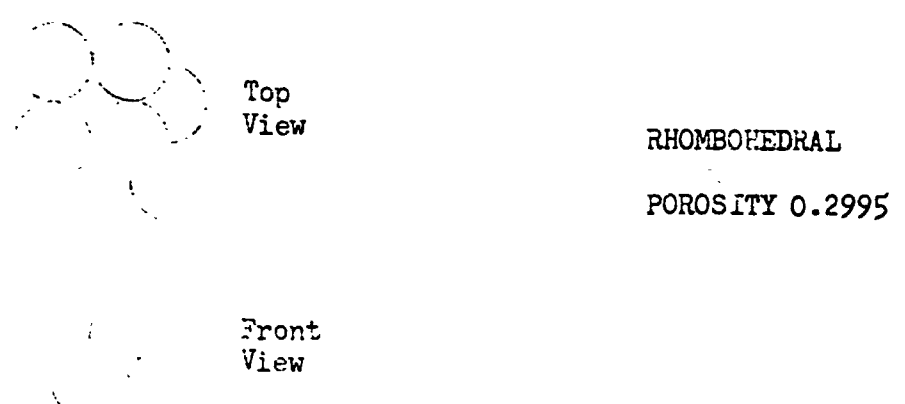
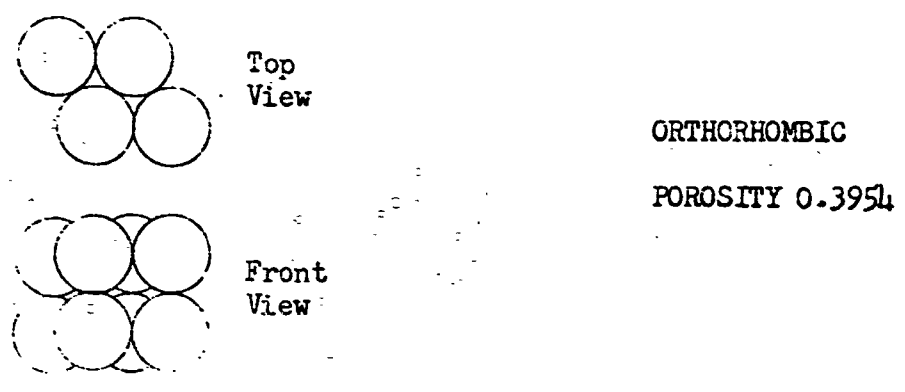
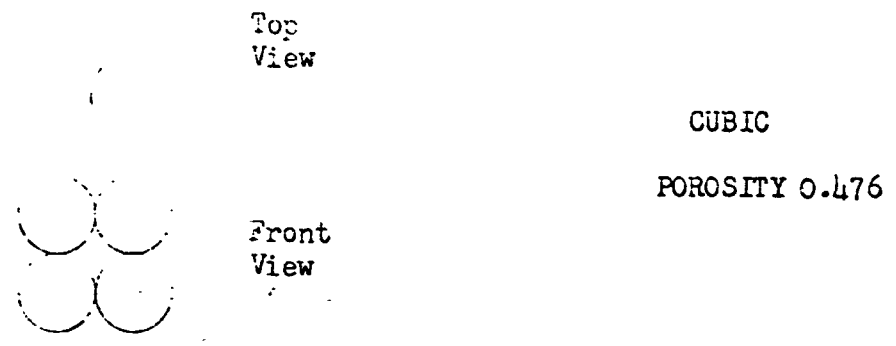


Figure 4

Some Alternate Arrangements of Regularly Packed Spheres

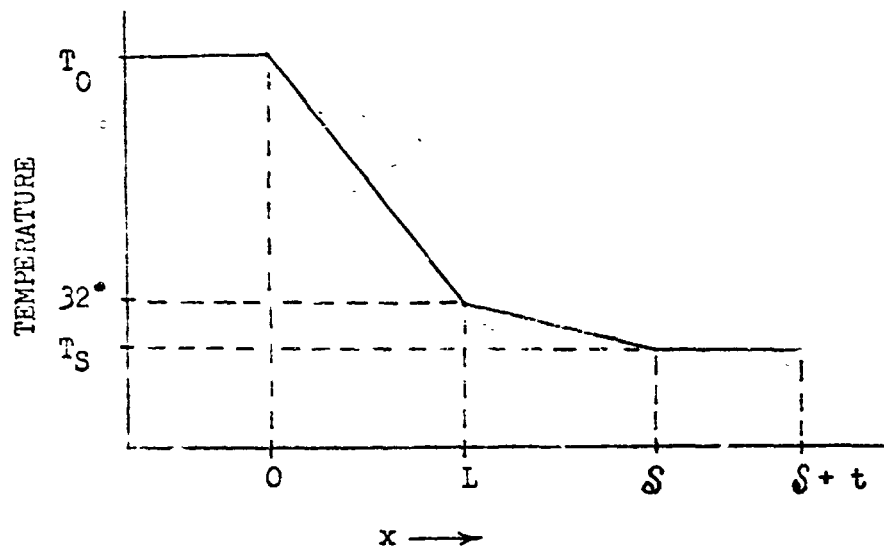
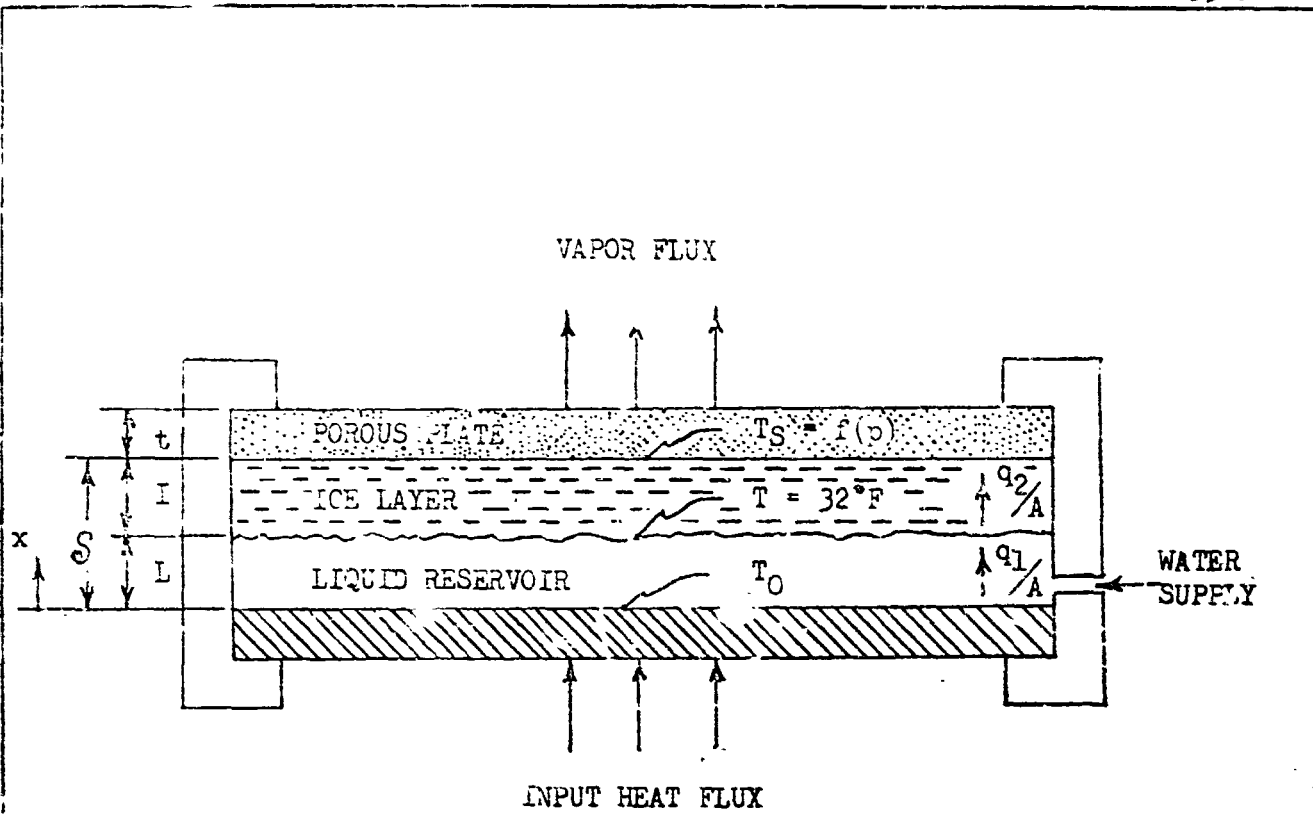


FIGURE 5

MODEL FOR ANALYSIS OF SUBLIMATION MECHANISM

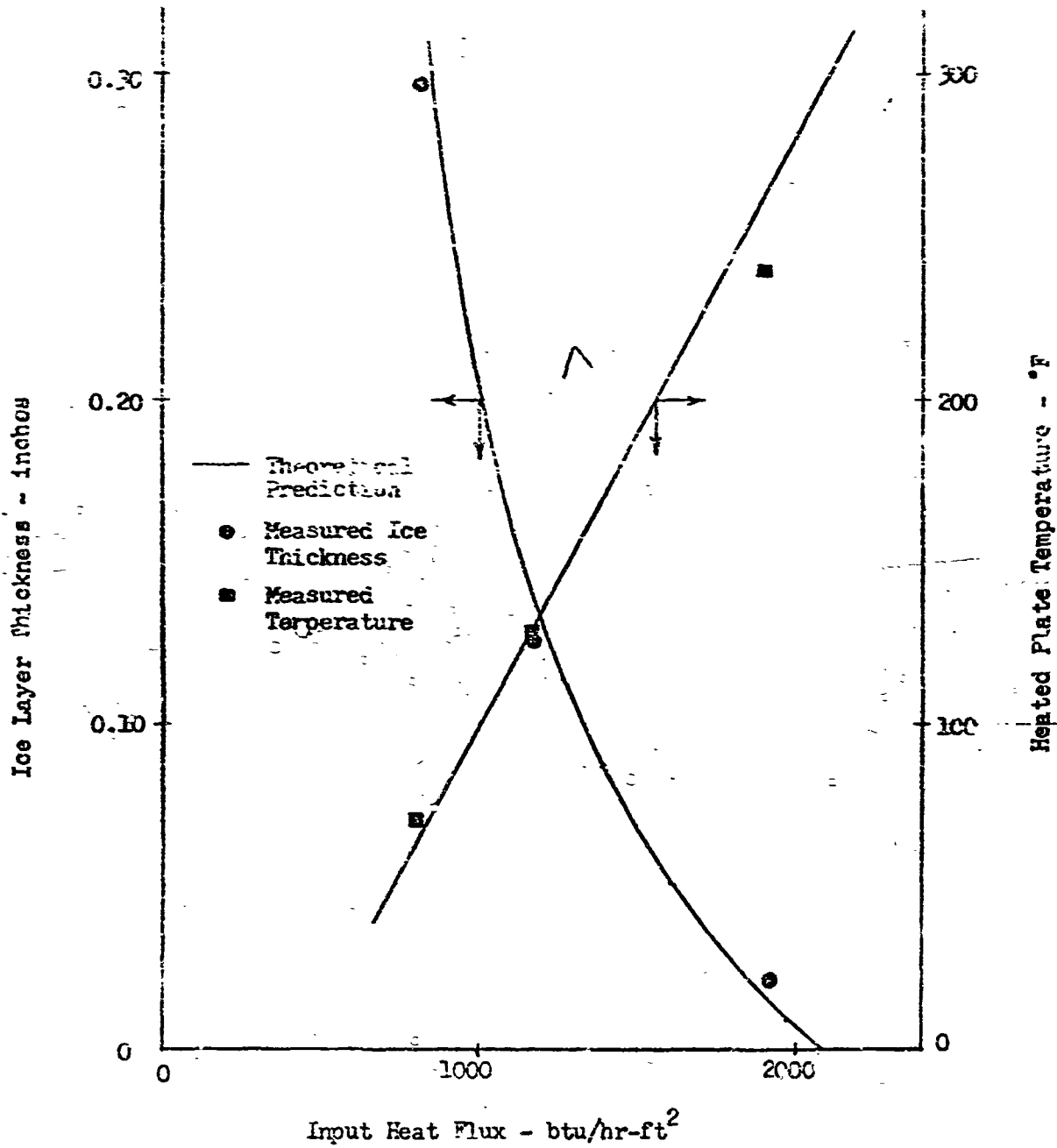


FIGURE 6

COMPARISON OF MEASURED ICE LAYER THICKNESS AND HEAT REJECTION PERFORMANCE WITH THEORETICAL PREDICTIONS FOR PLATE E OPERATING IN THE SUBLIMATION MODE

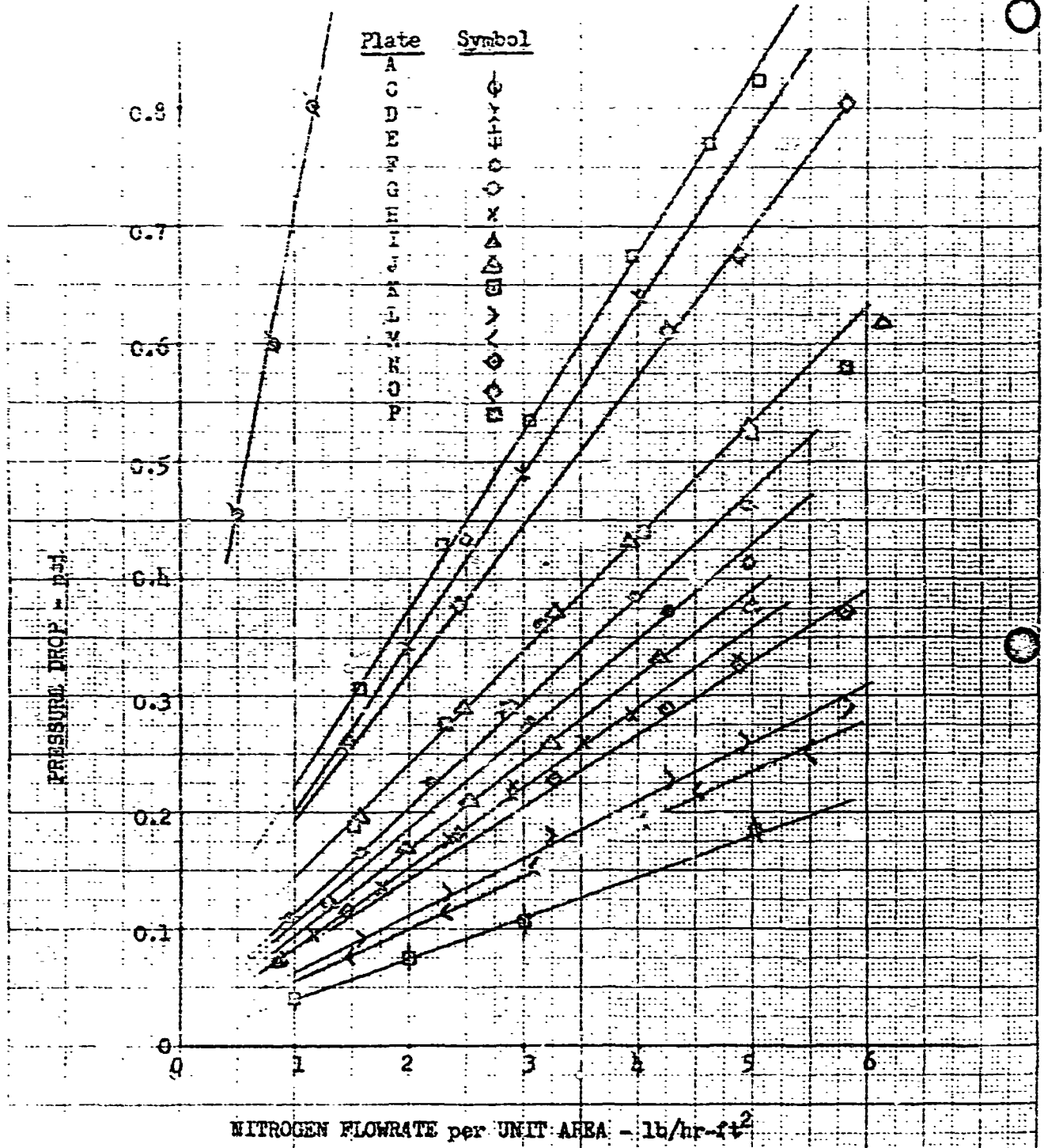


FIGURE 7

PORCUS PLATE FLOW CHARACTERISTICS AT SIMULATED OPERATING CONDITIONS
 EXIT PRESSURES OF 90 TO 1500 MICRONS OF MERCURY

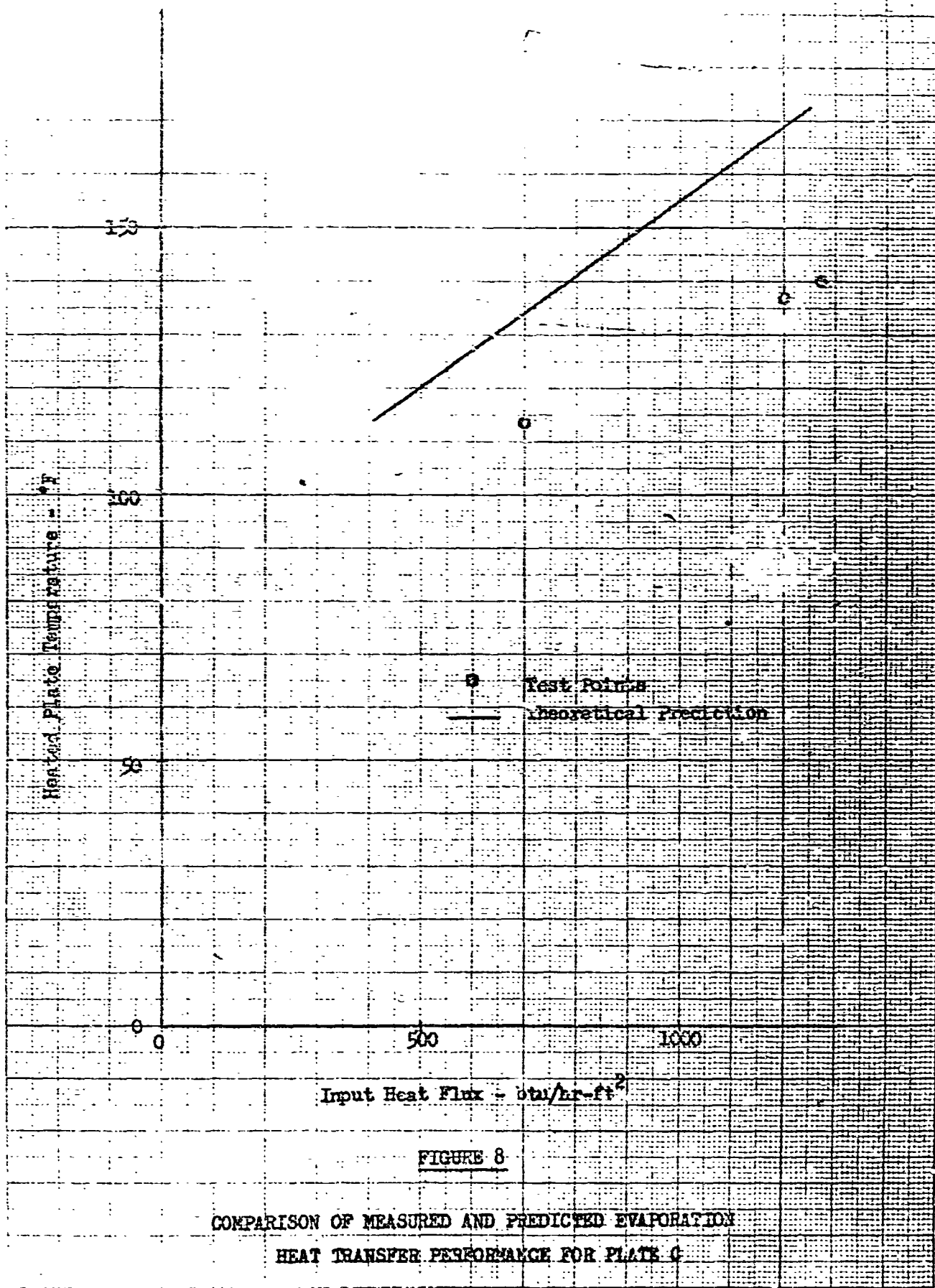


FIGURE 8

COMPARISON OF MEASURED AND PREDICTED EVAPORATION
HEAT TRANSFER PERFORMANCE FOR PLATE C

FOR SALES DIETZGEN BRASSI PAPER LUDWIG DIETZGEN GMBH MADE IN GERMANY MILLIMETER

EUGENE DIETZEN CO.
MADE IN U.S.A.
EUGENE DIETZEN CO. PAPER
MILLIMETER

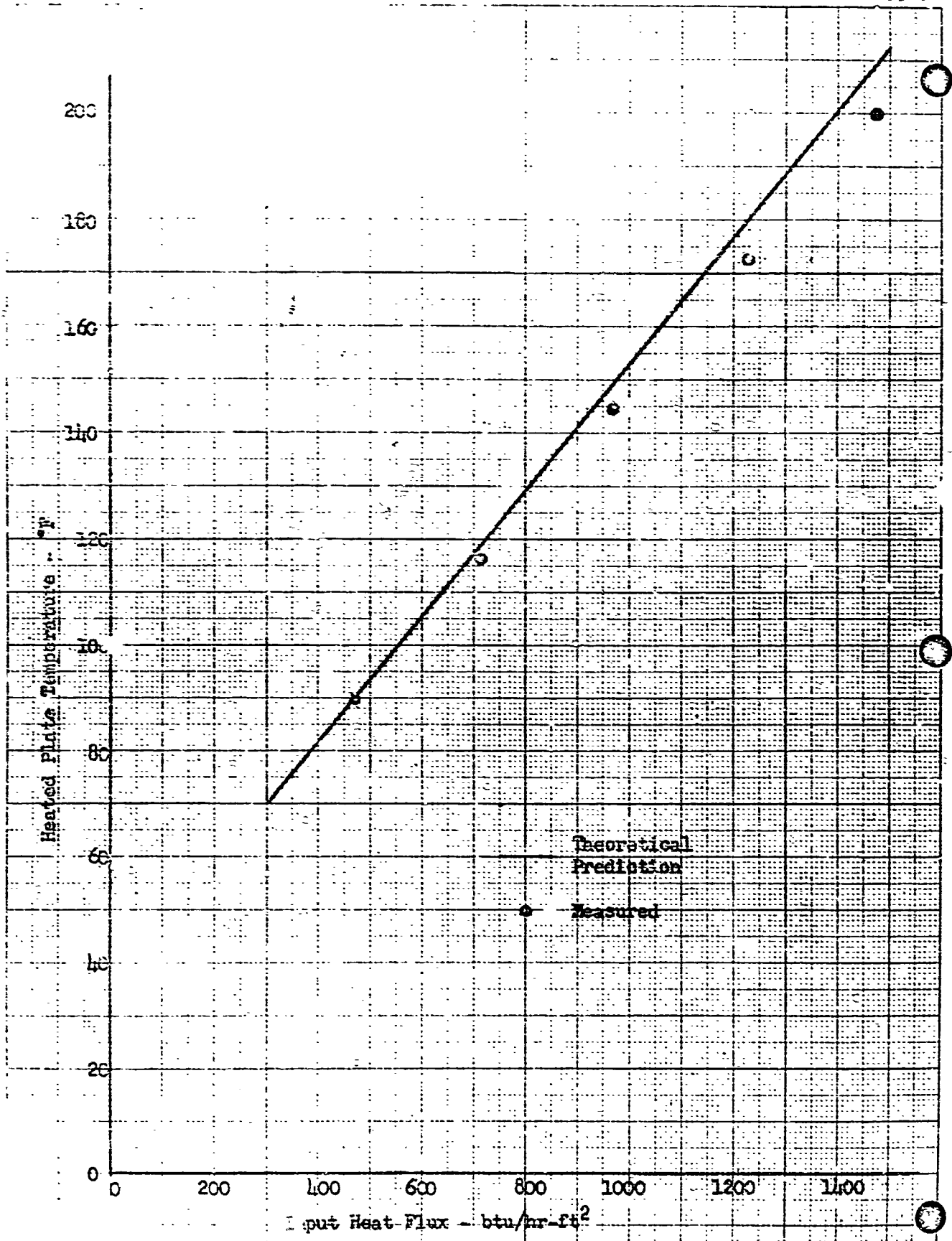


FIGURE 9
 Comparison of Measured and Predicted Heat Transfer Performance of
 Plate C Operating in the Mixed Mode

EUGENE D. STUBEN CO.
MAY 10, 1954

NO. 10-104 DIETRICH GRAPH PAPER
MILLIMETER

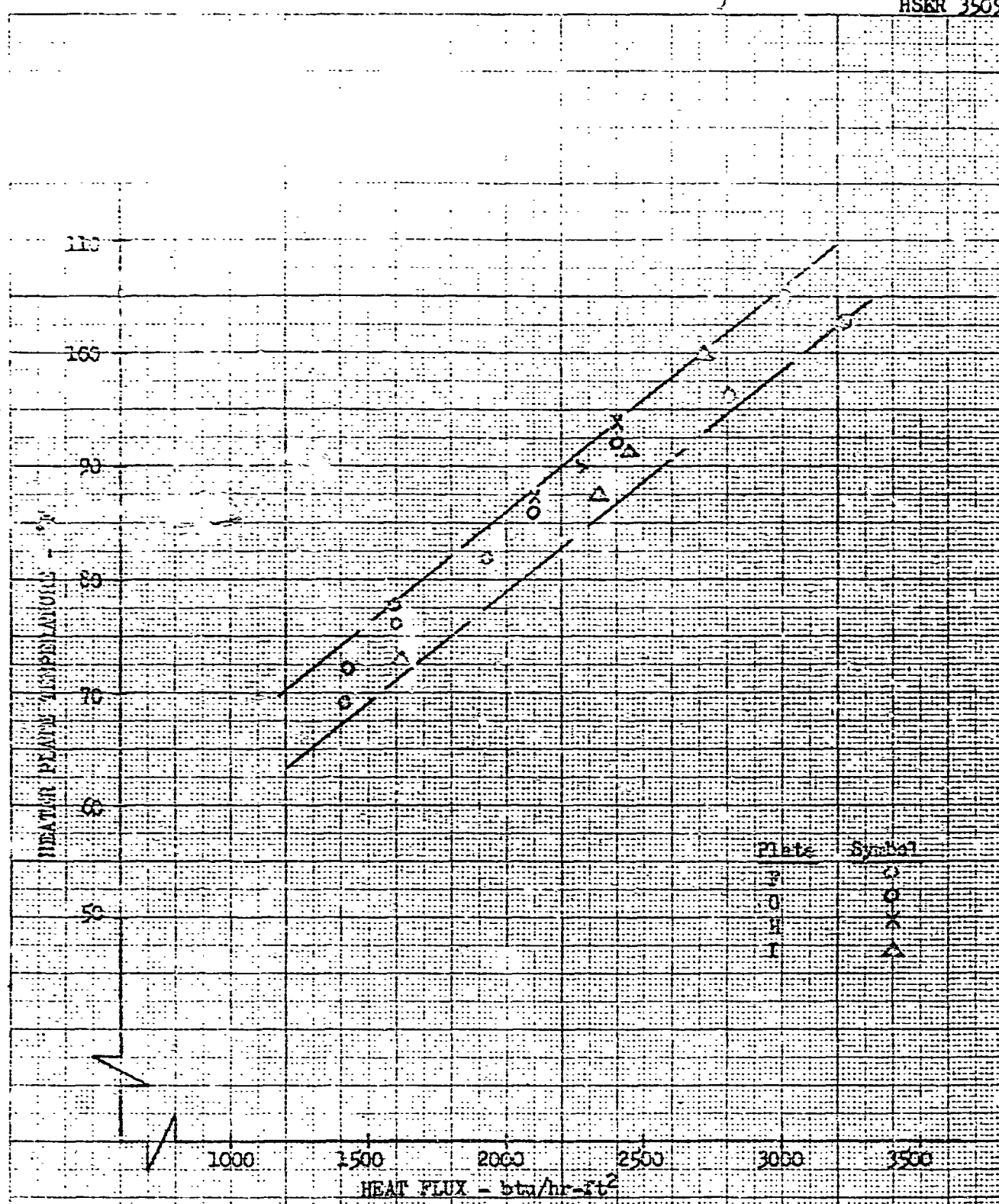
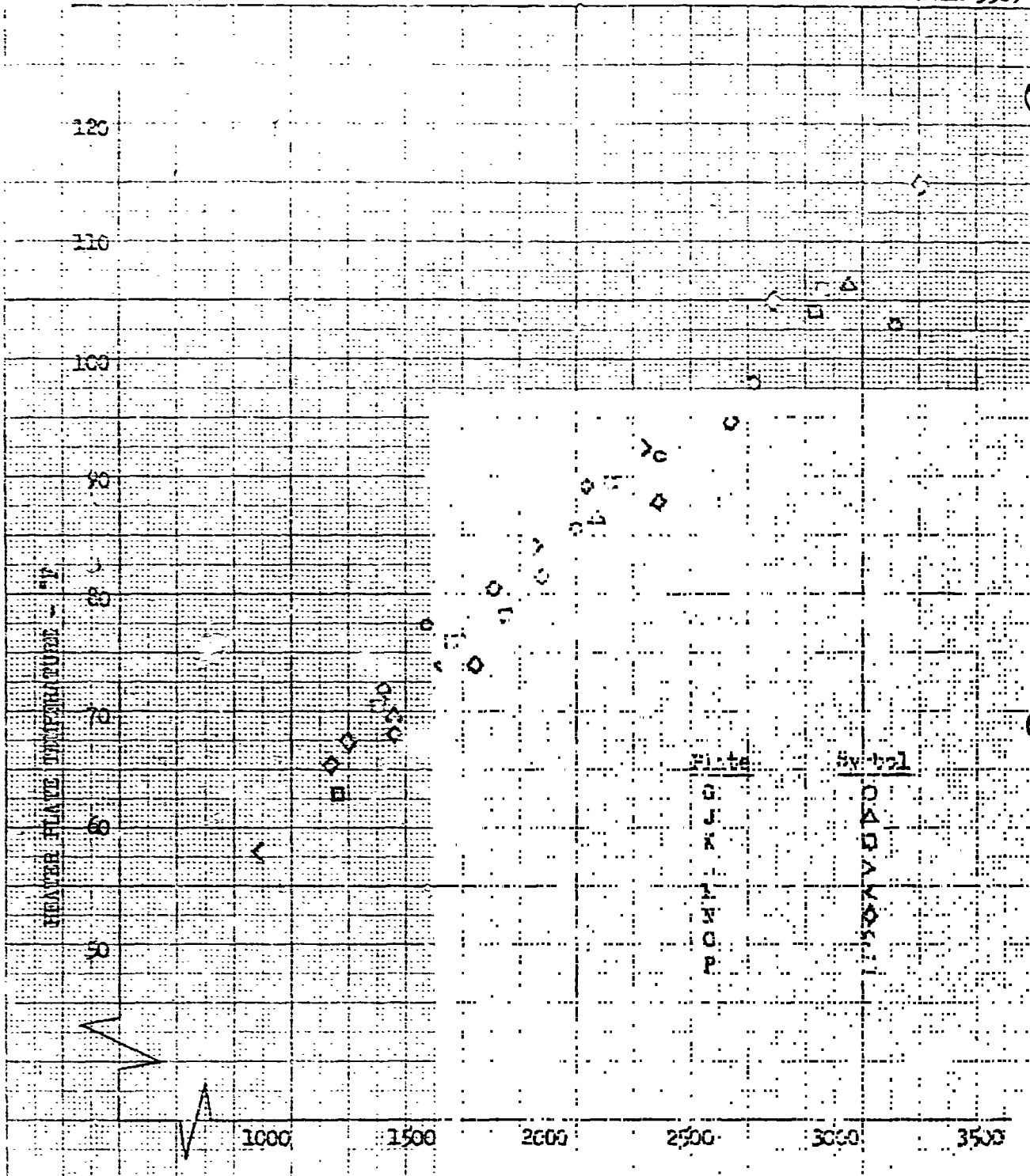


FIGURE 10
REPRODUCIBILITY OF HEAT TRANSFER PERFORMANCE FOR
POROUS PLATES MADE TO IDENTICAL SPECIFICATIONS



HEAT FLUX - BTU/IN²

REVERSE PLATE TEMPERATURE - °F

FIGURE 11

EFFECT OF PLATE CHARACTERISTICS ON PERFORMANCE

EUGENE DIEZEL CO. MADE IN U.S.A. DIEZEL GRAPH PAPER MILLIMETER

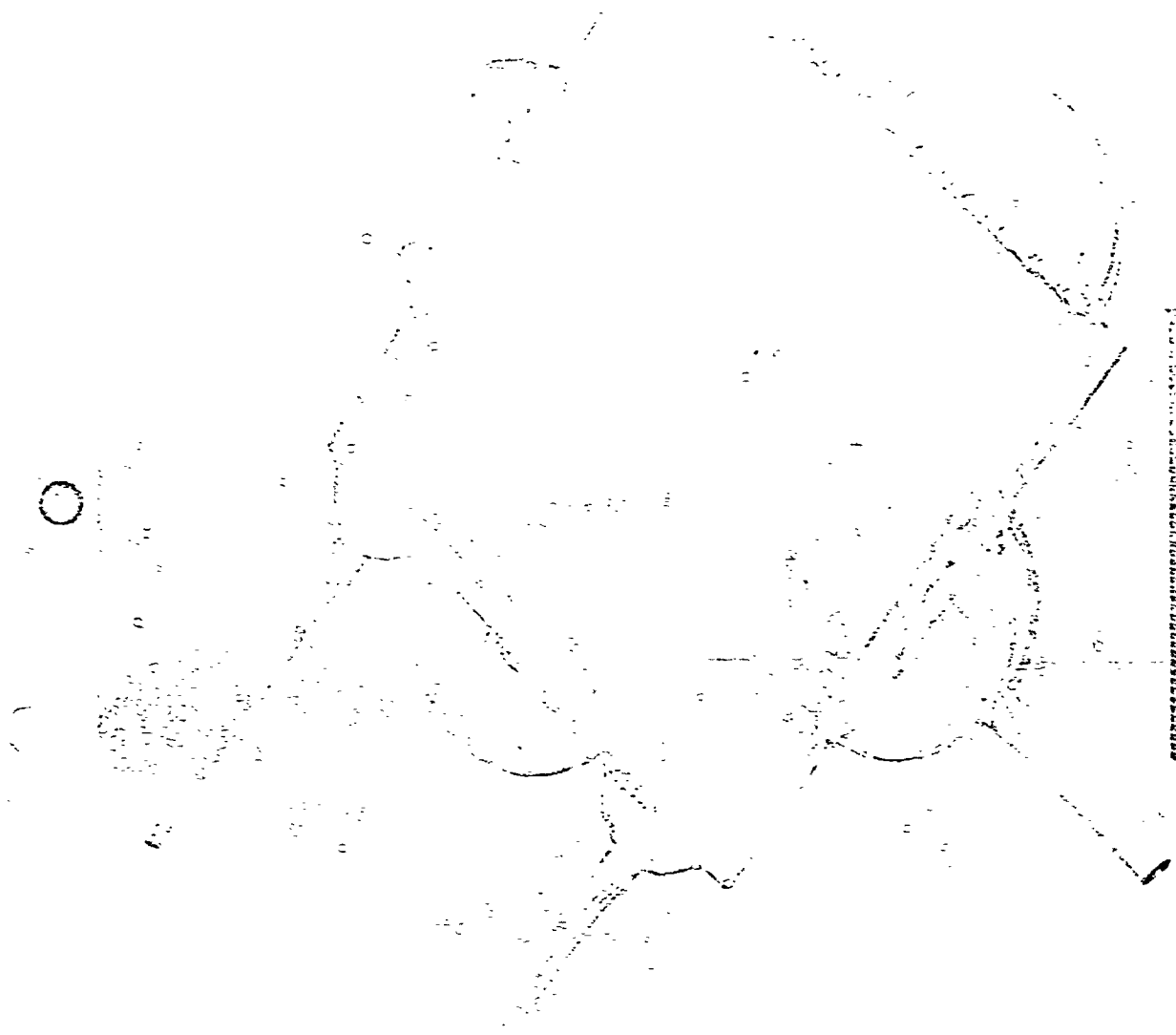
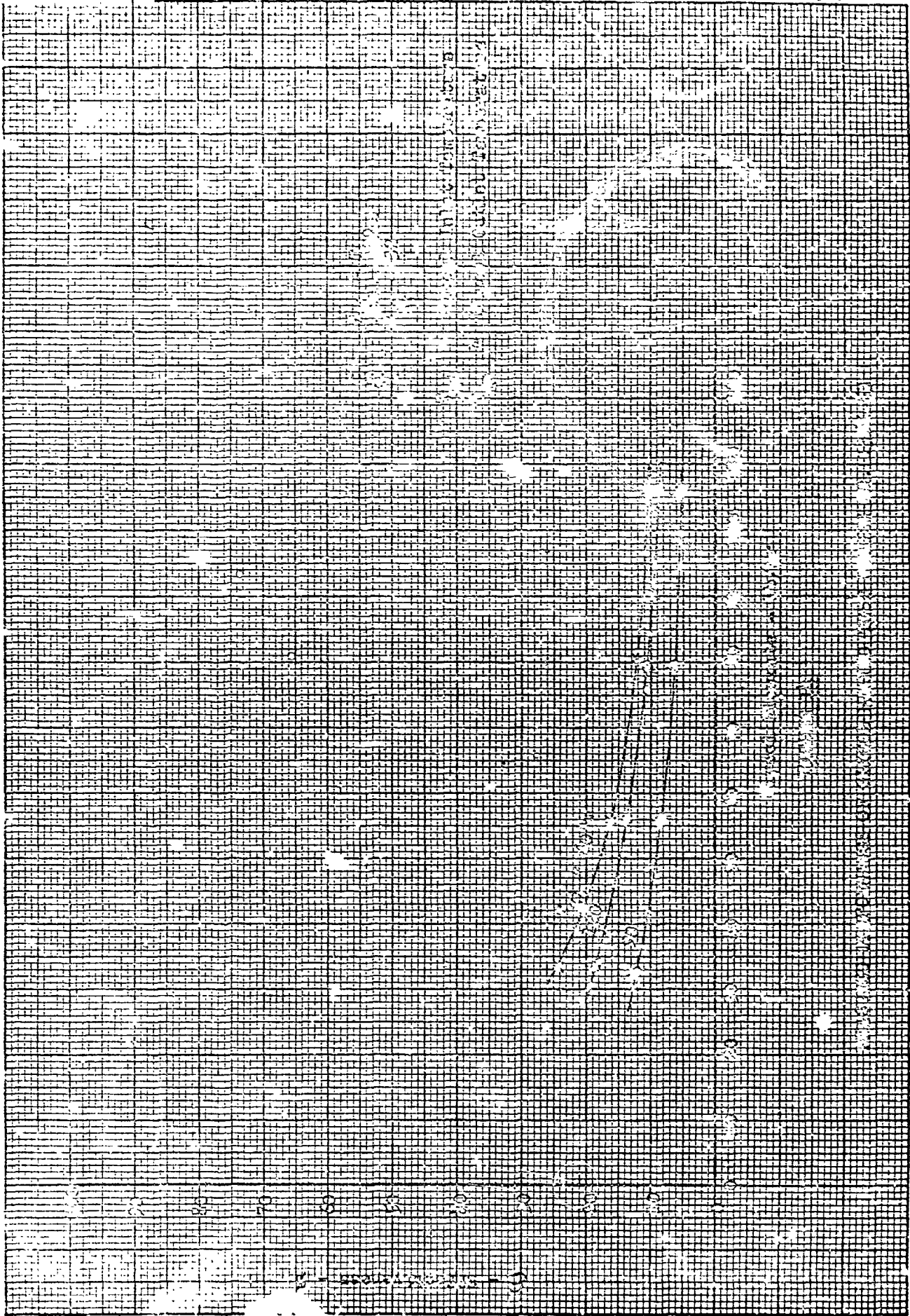


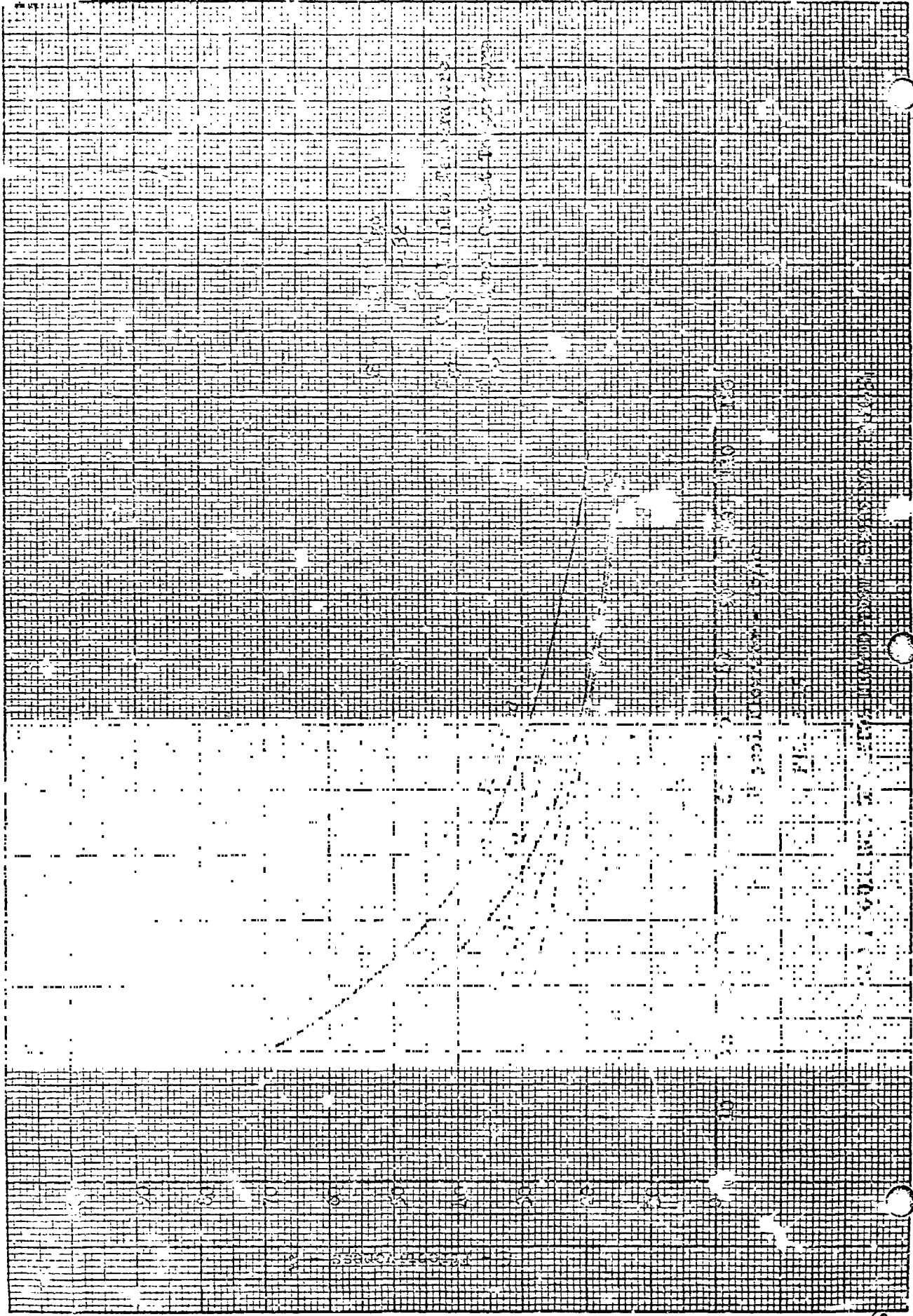
FIGURE 12 - Glycol Heated Porous Plate Water Boiler Test Module

FIGURE 12 - Glycol Heated Porous Plate Water Boiler Test Module

K^oΣ 10 X 10 TO THE 1/2 INCH 359-11
KEUFFEL & EBBER CO. MADE IN U.S.A.

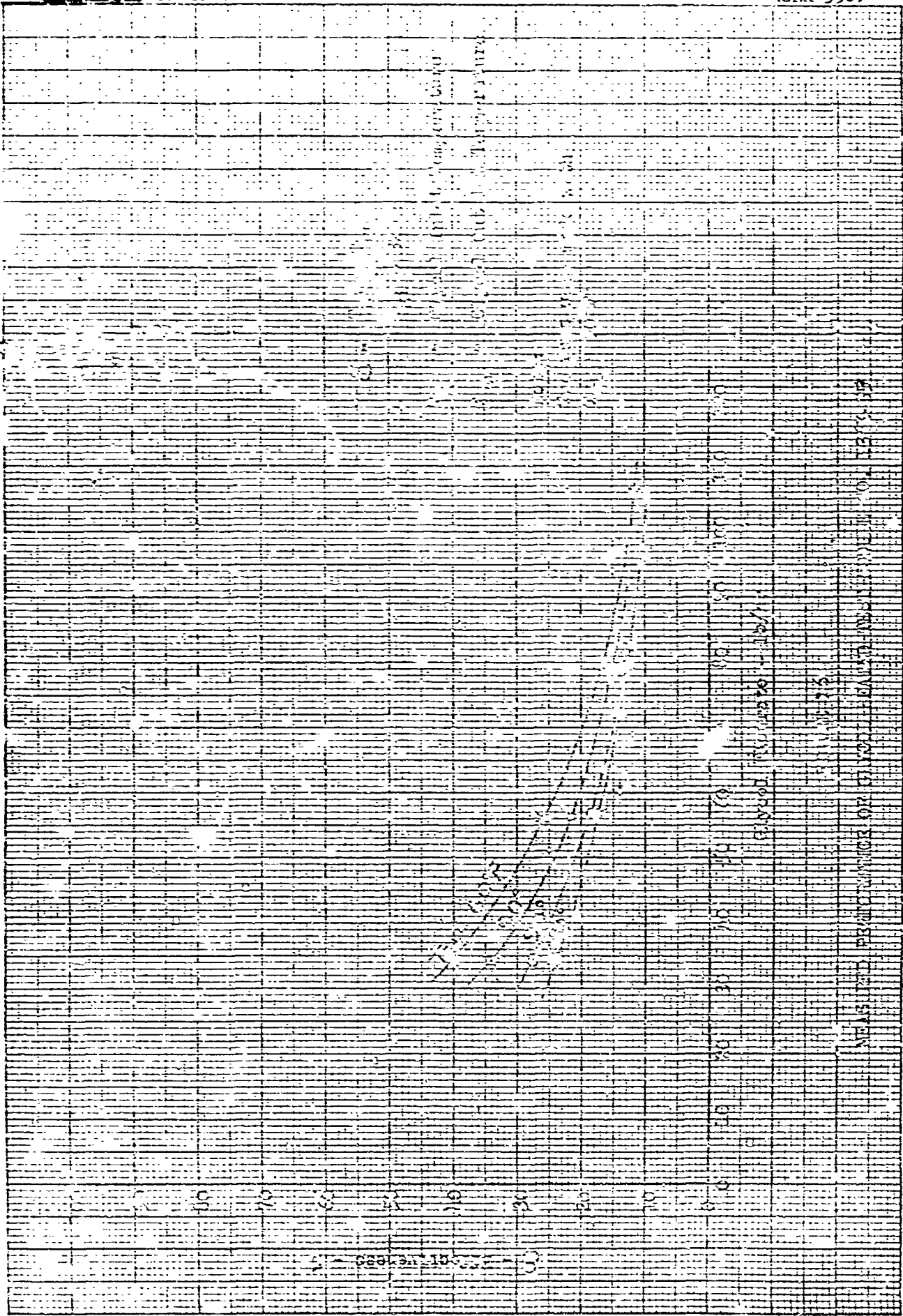


10 X 10 TO THE 1/2 INCH
NEUFEL & ESSER CO.
U.S.A.



OR BETTER COPY CONTACT THE DOCUMENT ORIGINAL

3509



KOE 10 X 10 TO THE 1/2 INCH 3509-11 MADE IN U.S.A. KRUPP & LEBER CO.

TABLE 1

Bubble Point and Water Retention Pressures
Before and After Degradation Tests

Plate	Water Retention Pressure - "Hga		Bubble Point Pressure "Hga						Test
	Initial "Hga	After Test "Hga	Initial			After Test			
			1st	10%	Full	1st	10%	Full	
Q	3.7	4.6	3.7	5.0	8.6	3.2	5.2	9.5	100 hour operation
R	5.4	5.4	3.7	5.0	8.1	4.6	6.6	9.4	Force Flush
R	5.4	5.6	4.6	6.6	9.4	5.5	6.0	8.0	651 hour soak
S	5.2	5.5	3.6	4.2	2.2	5.3	6.2	7.6	662 hour soak

TABLE 2

Performance of Porous Plates
During Degradation Tests

Plate	Test	Heater Plate Temperature at Constant Heat Flux									
		°F	Time	°F	Time	°F	Time hr.	°F	Time hr.	°F	Time
Q	100 hour operation	63	initial	62	25 hr	62	50	64	75	63	final 104 hr
R	force flush	64	initial	65	final						
R	soak	65	initial	66	100 hr	67	191	70.5	317	73	final 651 hr
S	soak	64	initial	66	100 hr	67	194	74	311	70	final 662 hr

Test Conditions:

1. Constant heat flux of 1533 Btu/hr-ft² used for all tests.
2. Water supply pressure maintained at 4-5 psia.
3. Test chamber pressure maintained at 50-100 microns of Hg.

TABLE 3

Run Sequence Compared to Effectiveness Level

Module No.	52		53		54		55	
	Run	ϵ^*	Run	ϵ	Run	ϵ	Run	ϵ
1	90	120	90	60	90	60	60	60
2	120	90	60	120	60	120	90	90
3	60	60	120	90	120	90	120	120

*Order of effectiveness from highest to lowest

TABLE 4

Average Effectiveness for Glycol Heated Modules

Module No.	Flow $\frac{\text{lb}}{\text{hr}}$	34	56	80	106
		52	20.9	14.2	10.8
53	17.9	12.6	10.0	8.1	
54	33.6	24.0	18.6	15.3	
55	31.	20.4	15.1	12.2	

TABLE 5

Performance of Phase IV Plates in Electrically Heated Modules

Module No.	Plate	Heat Flux BTU/hr-ft^2	Ambient Pressure PSIA	Water Feed Pressure PSIA	Heater Plate Temperature $^{\circ}\text{F}$
52	T	1533	0.0019	4.5	73
53	U	1533	0.0027	5.0	70
54	V	1533	0.00087	2.4	66
55	W	1533	0.00078	1.6	68

APPENDIX C

PLATE DESCRIPTION AND
PERFORMANCE DATA

TABLE 6

DESCRIPTION OF POROUS PLATES

PLATE	MATERIAL	THICKNESS	% DENSITY	PARTICLE SIZE DISTRIBUTION	PHASE
A	Stainless Steel	0.032	.615	-	II
B	Nickel	0.058	.745	-	II
C	Nickel	0.038	.74	-	II
D	Stainless Steel	0.033	.735	-	II
E	Teflon Impregnated Fiberglass	0.006	-	-	II
F	Nickel	0.061	61	25-37	III
G	Nickel	0.060	65	25-37	III
H	Nickel	0.055	63	25-37	III
I	Nickel	0.055	64	25-37	III
J	Titanium	0.052	62	25-37	III
K	Copper	0.064	66	25-37	III
L	Nickel	0.032	65	25-37	III
M	Nickel	0.063	55	25-37	III
N	Nickel	0.061	62	37-44	III
O	Nickel	0.056	76	25-37	III
P	Nickel	0.063	63	15-25	III
Q	Nickel	0.038	83	-	IIIb
R	Nickel	0.038	83	-	IIIb
S	Nickel	0.039	83	-	IIIb
T	Nickel	0.039	83	-	IV
U	Nickel	0.038	83	-	IV
V	Nickel	0.031	81	-	IV
W	Nickel	0.032	82	-	IV

TABLE 7

MEASURED WATER RETENTION, BUBBLE POINT, AND
PERMEABILITY OF POROUS PLATES USED

PLATE	BUBBLE POINT psi	WATER RETENTION psi	ΔP @ lb/Hr-ft ² Vacuum Discharge
A	-	0.069	0.050
B	-	0.73	-
C	-	5.4	0.70
D	-	1.33	0.20
E	0.36	1.18	0.040
F	2.1	0.172	0.105
G	2.4	0.163	0.115
H	2.1	0.117	0.085
I	2.2	0.063	0.090
J	2.8	0.145	0.150
K	3.7	0.217	0.245
L	2.1	0.397	0.055
M	1.6	0.271	0.050
N	1.9	0.181	0.085
O	2.4	0.885	0.205
P	2.6	0.452	0.150
Q	1.81	1.81	0.25 *
R	1.81	2.64	0.20 *
S	1.76	2.55	0.25 *
T	2.6	2.75	0.36 *
U	2.7	2.7	0.30 *
V	1.9	-	0.24 *
W	1.8	-	0.16 *

TABLE 8

SUMMARY OF PERFORMANCE DATA FOR PHASE II

VERIFICATION COOLING MECHANISMS

No.	Plate	Spacing	Heat Flux Btu/Hr/ft ²	Ambient Pressure psia	Water Feed Pressure psia	Porous Plate Temp. °F	Heater Plate Temp. °F	Ice Layer Thickness in.
1	A	.5	813	0.00082	2.4	16.5	58.7	.387
2	A	.5	940	0.00118	2.4	16.7	90.8	.245
3	B	.3	945	0.00078	4.4	-	97.3	-
4	B	.3	1315	0.00102	4.4	-	125.1	-
5	B	.3	1705	0.00118	4.4	-	150.8	-
6	C	.5	470	0.00082	4.0	33.7	89.7	-
7	C	.5	710	0.00078	4.0	34	116.5	-
8	C	.5	970	0.00092	4.0	34.2	144.7	-
9	C	.5	1230	0.00098	7.8	32	172.9	-
10	C	.5	1475	0.00098	15.2	31.8	199.3	-
11	C	.3	590	0.00108	5.8	31.9	74.2	-
12	C	.3	1280	0.00176	5.8	32	122.5	-
13	C	.3	1800	0.00176	8.3	32.1	156	-
14	C	.3	694	0.57	2.9	-	113.6	0
15	C	.3	1200	0.57	3.9	-	136.1	0
16	C	.3	1265	0.57	4.9	-	139.9	0
17	D	.5	417	0.00135	3.8	30.7	77	.065
18	D	.5	420	0.00174	3.8	30.5	78	.067
19	D	.5	475	0.00147	3.8	28.9	81.5	.073
20	D	.5	580	0.00193	3.8	31.5	100	.025
21	D	.5	610	0.00088	3.8	33.7	102.5	.01
22	D	.5	690	0.00118	3.8	31.2	110.5	.01
23	E	.5	800	0.00098	2.2	-	72.8	.296
24	E	.5	1166	0.00098	2.2	-	123.6	.126
25	E	.5	1920	0.00118	2.2	-	239	.03
26	E	.3	635	0.00088	2.0	-	43.4	.23
27	E	.3	710	0.00121	2.0	-	52.4	.17
28	E	.3	825	0.00118	2.0	-	82.5	.05

TABLE 9

SUMMARY OF PERFORMANCE DATA FOR PHASE III
INFLUENCE OF PLATE VARIABLE

No.	Plate	Heat Flux Btu/Hr-Ft ²	Ambient Pressure psia	Water Feed Pressure psia	Heater Plate Temperature °F
1	F	1420	0.0077	2.6	68
2	F	1600	0.0058	3.0	75.5
3	F	1930	0.0058	2.6	81.5
4	F	2140	0.0058	2.4	90.5
5	F	2810	0.0048	2.4	102
6	F	3000	0.0058	2.0	105
7	G	1420	0.0019	1.6	71
8	G	1590	0.0018	1.4	77
9	G	2100	0.0019	1.5	86
10	G	2390	0.0024	1.5	93
11	G	3220	0.0023	2.4	105
12	H	1650	0.0019	1.9	71.5
13	H	2000	0.0021	1.6	81
14	H	2010	0.0058	1.6	88
15	H	2380	0.0027	1.5	97
16	I	1620	0.0019	2.0	73
17	I	2020	0.0009	1.6	77
18	I	2340	0.0018	1.6	87
19	I	2430	0.0018	1.5	93
20	I	2700	0.0018	1.4	102
21	J	1450	0.0013	2.0	70
22	J	2150	0.0014	1.8	86
23	J	2640	0.0013	1.8	95
24	J	3060	0.0016	1.8	106
25	J	3740	0.0017	4.6	120
26	J	4110	0.0019	4.8	127

Table 9
Continued on
next page --

TABLE 9
(continued)

No.	Plate	Heat Flux Btu/Hr-ft ²	Ambient Pressure psia	Water Feed Pressure psia	Heat Plate Temperature °F
27	K	1250	0.0009	2.4	63
28	K	1545	0.0010	2.2	68
29	K	1855	0.0014	2.2	76
30	K	2390	0.0018	1.8	87
31	K	2920	0.0058	2.0	104
32	L	1440	0.0023	1.0	71
33	L	1690	0.0029	1.8	77
34	L	1975	0.0041	1.4	84
35	L	2260	0.0027	1.0	93
36	M	950	0.0023	1.6	58
37	M	1600	0.0024	1.8	74
38	N	1230	0.0023	1.8	66
39	N	1440	0.0025	1.6	69
40	N	1730	0.0033	1.7	75
41	N	1800	0.0029	1.7	81
42	N	2380	0.0029	1.5	88
43	O	1280	0.0031	1.5	68
44	O	1680	0.0025	1.3	76
45	O	1980	0.0033	1.3	82
46	O	2140	0.0031	1.2	90
47	O	2880	0.0027	1.7	106
48	O	3300	0.0027	2.1	116
49	O	3580	0.0058	1.9	123
50	P	1400	0.0031	1.8	70
51	P	1685	0.0027	1.7	76
52	P	1970	0.0031	1.8	84
53	P	2220	0.0031	1.6	89
54	P	2720	0.0033	1.5	98
55	P	2930	0.0039	1.6	107
56	P	3540	0.0031	2.0	120

HISTORY AND TEST DATA FROM
INVESTIGATION OF
PERFORMANCE DETERIORATION OF
NICKEL POROUS PLATES

HISTORY OF PLATE Q

1. Initial Inspection
 - a. Measured bubble point pressure
 - b. Measured water retention pressure
 - c. Measured permeability at atmospheric exit pressure
 - d. Measured permeability at simulated operating pressures
 - e. Established initial performance reference
2. Operated plate continuously in electrically heated module for 100 hours at the following conditions:

Heat Flux - 1500 Btu/hr-ft²
Water Pressure - 4.2 psia
3. Back flushed plate with ultra-pure effluent for contamination analysis.
4. Final Inspection
 - a. Measured bubble point pressure
 - b. Measured water retention pressure
 - c. Measured permeability at atmospheric exit pressures
 - d. Measured permeability at simulated operating pressures
 - e. Conducted extraction analysis of matter deposited on plate during 100 hours of operation

HISTORY OF PLATE R

1. Initial Inspection
 - a. Measured bubble point pressure
 - b. Measured water retention pressure
 - c. Measured permeability at atmospheric exit pressure
 - d. Established initial performance reference
2. Force flushed 7.2 liters of distilled water through plate (same amount consumed by plate Q in 100 hours operation at 1500 Btu/hr-ft²)
3. Intermediate Inspection
 - a. Checked performance
 - b. Measured water retention pressure
 - c. Measured bubble point pressure
 - d. Measured permeability at atmospheric exit pressure
4. Soaked in distilled water in a covered but not air tight glass container for 651 hours and checked performance at various times.

HISTORY OF PLATE R (continued)

5. Final Inspection

- a. Checked performance
- b. Measured bubble point pressure
- c. Measured water retention pressure
- d. Measured permeability at atmospheric exit pressure.

HISTORY OF PLATE S

1. Initial Inspection

- a. Measured water retention pressure
- b. Measured bubble point pressure
- c. Measured permeability at atmospheric exit pressure
- d. Established initial performance reference

2. Soaked plate in distilled water, boiled to remove any air, in a closed glass container with a nitrogen atmosphere above the water for 662 hours and checked performance periodically.

3. Final Inspection

- a. Checked performance
- b. Measured bubble point pressure
- c. Measured water retention pressure
- d. Measured permeability at atmospheric exit pressure

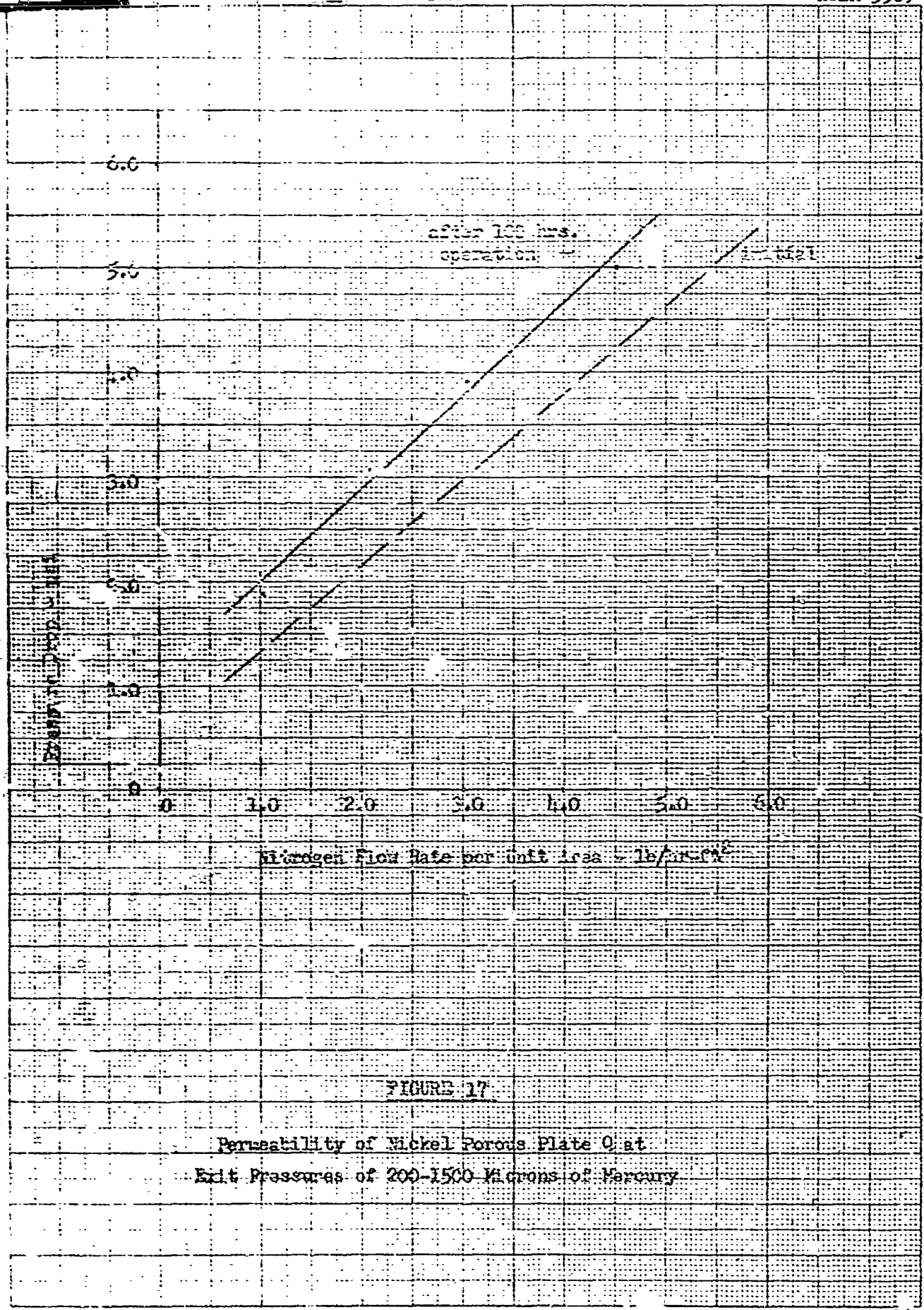


FIGURE 17

Permeability of Nickel Porous Plate C at
Exit Pressures of 200-1500 Microns of Mercury

EUGENE PIETZORN CO.
MADE IN U. S. A.

1.0 MM. DIAMETER GRAPH PAPER
MULTIMETER

EUSIFNE DUTZGEN CO.
MADE IN U. S. A.

50 MIL x DUTZGEN GRADE PAPER
MILLIMETER

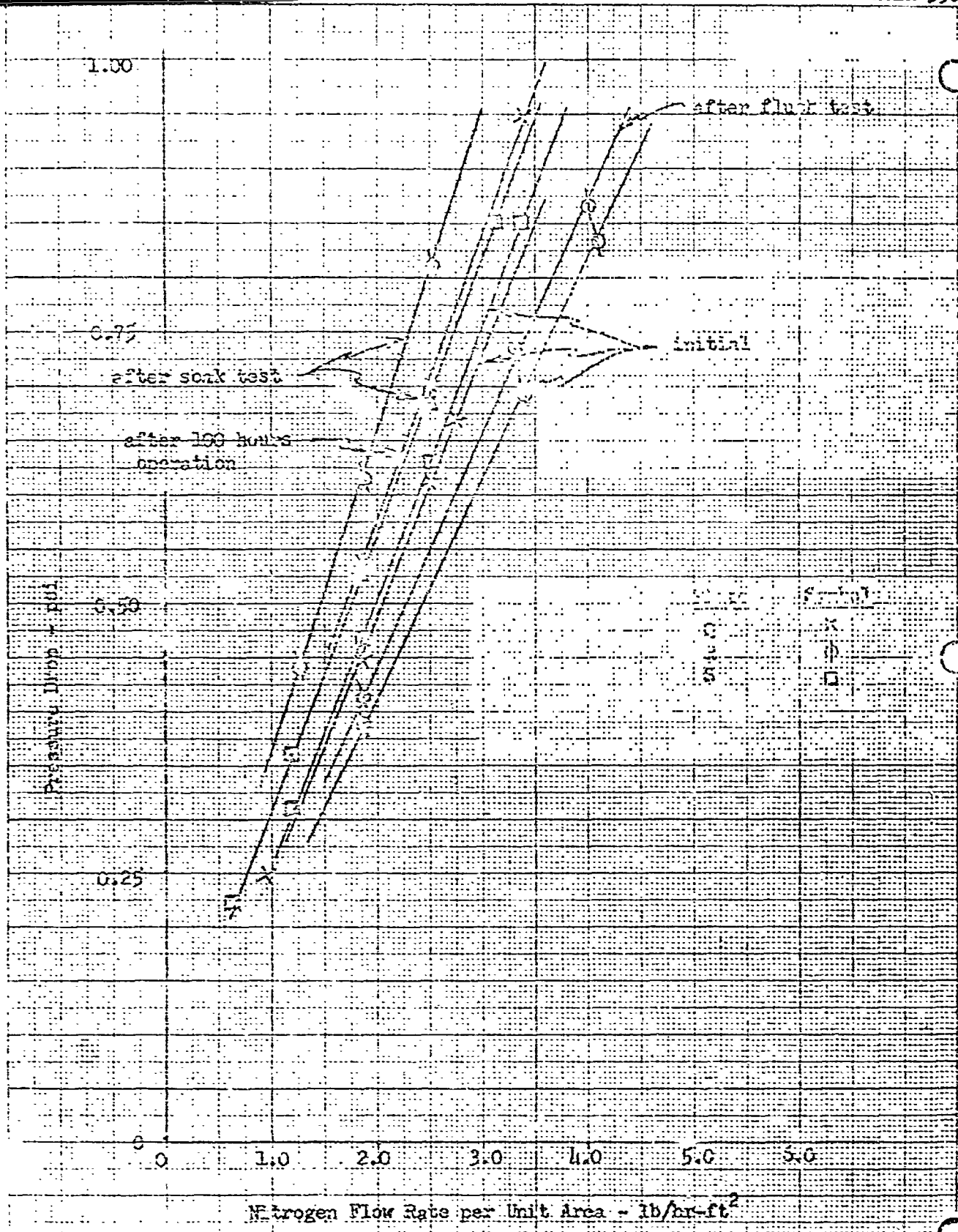


FIGURE 16
 Permeability of Nickel Porous Plates Before and After Degradation in
 Performance tests

TABLE 10
ANALYSIS OF DISTILLED WATER BEFORE USED IN THE VARIOUS DEGRADATION TESTS

pH	3.7
Carbonates	Slight trace
Chlorides	None
Sulfates	None
Fluoride	None in 50 ml.
Aluminum	None
Nickel	None
Oxygen	1/10 ppm
NH ₃	None
NO ₂	None
NO ₃	0.016 ppm
Chloroform Extract (Anything which dissolves in chloroform)	6 ppm
Total Solids	9 ppm
Fixed Solids	8 ppm
Bacteria Count:	
By membrane filter	0 ppm
By plate count	4 ppm

TABLE 11
ANALYSIS OF WATER AFTER USED IN TESTS

A. Triple Distilled Water Effluent After Back Flushed Through Nickel Porous Plate Q	
pH	7.0
Carbonates	Slight Trace
Chlorides	None
Sulfates	None
Particle Count	
Total Solids	27.6 ppm
Bacteria Count	None
B. Distilled Water in which Nickel Porous Plate R was Soaked for 651 Hours in an Open Glass Container	
pH	6.5
Carbonates	Very Slight Trace
Chlorides	None
Sulfates	None
Particle Count	
Total Solids	(not made)
Bacteria Count	Many colonies of gram negative bacillus, some gram positive bacillus, and some yeast.
C. Distilled water in which Nickel Porous Plate S was Soaked for 662 Hours in a Closed Glass Container with a Nitrogen Atmosphere over the Water	
pH	7.0
Carbonates	Very Slight Trace
Chlorides	None
Sulfates	None
Particle Count	
Total Solids	(not made)
Bacteria Count	Few Colonies of Gram negative Bacillus and Occasional Yeast

TABLE 12

PERFORMANCE DATA PHASE IV --
TRANSPORT FLUID HEATED MODULES

MODULE NO.	GLYCOL SIDE				WATER SIDE		AMBIENT PRESSURE microns
	Flow ml/min	Pressure psia	T _{in} °F	T _{out} °F	Flow lb/min	Supply Pressure psia	
52	800	11.8	93.6	87.0	7.18	5.4	98
52	800	11.9	92.2	85.4	7.17	5.3	97
52	600	12.2	91.8	85.0	6.40	5.3	96
52	600	12.1	90.8	84.0	6.90	5.2	90
52	400	12.9	89.5	81.2	5.51	5.2	82
52	405	13.1	88.8	80.8	5.40	5.2	82
52	205	11.4	88.1	76.8	1.81	5.2	80
52	400	7.0	89.3	82.0	5.45	5.0	130
52	800	11.1	120.7	114.0	11.2	5.0	92
52	600	10.6	119.0	108.9	9.84	4.9	110
52	395	9.2	117.7	107.2	8.51	4.8	110
52	400	9.4	121.0	105.7	--	4.5	120
52	205	11.6	118.2	98.2	11.4	4.5	110
52	195	11.3	118.6	97.5	11.0	4.5	110
52	795	12.0	62.2	60.3	2.49	5.4	500
52	800	12.2	61.9	59.9	2.37	5.4	700
52	795	12.3	61.1	59.0	2.33	5.5	60
52	600	8.0	61.2	58.4	--	5.4	55
52	605	8.2	60.5	57.7	2.15	5.4	55
52	400	10.0	60.6	57.2	2.10	5.3	47
52	395	10.0	60.9	57.2	2.11	5.4	47
52	200	9.4	62.2	56.6	2.04	5.5	47
52	195	9.4	61.6	56.1	2.07	5.5	46
53	800	12.4	90.5	87.6	4.14	4.7	110
53	805	12.2	90.5	87.8	4.01	4.6	110
53	600	11.5	90.2	86.4	3.72	4.7	110
53	600	11.5	91.9	88.1	--	4.6	105
53	400	9.2	92.4	87.1	3.37	4.6	110
53	395	9.2	92.1	87.0	--	4.6	110
53	195	12.9	92.0	84.6	--	4.6	110
53	190	11.9	91.1	84.6	3.06	4.6	110
53	795	12.6	67.3	65.1	4.69	5.5	80
53	795	12.9	65.1	62.1	3.74	5.5	80
53	795	13.1	62.8	60.0	3.17	5.5	80
53	595	10.5	62.4	57.9	2.84	5.5	70
53	605	10.9	62.6	59.2	2.61	5.5	65
53	395	7.5	61.9	57.8	2.74	5.5	65
53	395	7.5	62.5	57.8	--	5.5	65
53	195	7.9	62.0	55.0	2.29	5.5	75
53	195	7.8	62.1	54.7	2.25	5.4	75
53	300	9.7	124.7	116.6	10.9	5.1	25
53	800	9.7	124.6	116.5	--	5.1	20
53	600	9.3	126.7	116.8	10.1	5.0	20
53	600	9.3	123.7	113.7	9.42	4.9	22

TABLE 12
(continued)

MODULE NO.	GLYCOL SIDE				WATER SIDE		AMBIENT PRESSURE microns
	Flow ml/min	Pressure psia	T _{in} °F	T _{out} °F	Flow lb/min	Supply Pressure psia	
53	400		121.6	109.5	8.43	4.8	25
53	400		120.5	108.6	--	4.8	25
53	195	9.2	118.0	102.1	7.20	4.5	27
53	195	9.2	115.9	100.2	6.87	4.5	27
54	800	15.4	93.5	81.2	12.13	5.0	35
54	800	15.4	92.7	83.6	11.92	4.8	35
54	600	9.3	91.8	80.6	10.45	5.5	35
54	600	9.4	91.3	79.7	10.87	5.5	30
54	400	5.5	90.8	77.3	9.50	5.4	26
54	400	5.1	90.9	77.4	9.34	5.4	36
54	200	5.1	90.8	71.1	8.05	5.2	34
54	200	5.8	90.2	70.7	8.00	5.3	43
54	800	11.0	62.5	57.5	5.54	5.0	80
54	800	11.0	61.0	56.4	5.34	4.7	75
54	600	6.8	62.1	56.7		5.4	75
54	600	6.6	62.2	56.5	4.31	5.2	72
54	400	3.2	62.9	55.1	4.94	5.3	70
54	400	3.4	62.6	54.6	4.47	5.25	70
54	200	2.8	63.4	50.5	--	5.0	72
54	700	2.8	63.5	50.6	3.78	5.1	72
54	800	13.1	115.6	103.1	17.1	4.1	160
54	800	12.9	118.0	105.4	16.6	5.0	160
54	800	12.6	119.1	106.6	16.5	4.8	160
54	600	7.8	117.7	102.0	14.7	4.6	150
54	600	7.8	118.2	102.8	13.6	5.4	160
54	400	7.1	115.8	96.1	12.9	5.3	140
54	400	7.2	117.7	97.8	13.1	5.1	140
54	200	6.3	120.1	92.0	--	5.1	130
54	200	6.3	120.5	91.7	12.7	5.2	140
55	178	3.8	60.5	48.6	3.52	4.6	65
55	199	4.0	61.0	49.6	3.25	4.6	66
55	199	4.0	61.2	50.1	3.45	4.6	66
55	399	3.7	58.7	51.9	3.79	4.6	66
55	398	3.7	60.2	52.6	3.70	4.6	69
55	590	5.5	59.3	54.2	3.55	4.6	75
55	595	5.2	59.6	54.5	4.23	4.6	75
55	610	5.1	59.0	54.6	4.26	4.1	70
55	199	4.2	93.0	73.1	7.98	4.2	95
55	200	4.2	93.3	73.6	7.61	4.2	100
55	201	13.2	93.5	76.7	6.52	4.5	82
55	200	13.2	92.6	75.6	6.45	5.1	90
55	200	13.4	93.1	76.4	6.56	4.8	80
55	400	8.7	92.5	81.7	6.83	4.6	88
55	400	8.6	91.4	81.4	6.78	4.5	88
55	600	14.9	92.0	84.0	7.31	5.0	92
55	600	14.8	90.5	83.4	7.05	4.8	90

TABLE 12
(continued)

MODULE NO.	GLYCOL SIDE				WATER SIDE		AMBIENT PRESSURE microns
	Flow ml/min	Pressure psia	T _{in} °F	T _{out} °F	Flow lb/min	Supply Pressure psia	
55	800	13.0	92.1	86.4	7.25	4.5	90
55	800	13.2	89.6	84.2	7.13	5.0	90
55	202	12.0	93.2	71.3	6.85	4.7	85
55	198	9.9	94.1	74.5	7.31	4.3	100
55	460	5.0	92.4	79.3	8.35	4.3	110
55	398	5.0	91.7	79.2	7.83	4.4	100
55	600	8.2	92.3	82.8	8.71	5.0	100
55	600	8.2	91.8	82.6	8.63	5.0	110
55	800	14.5	92.3	82.7	9.32	4.6	110
55	800	14.5	93.0	82.8	9.23	4.7	110
55	800	8.0	60.8	57.6	3.45	4.5	66
55	800	7.9	62.1	57.9	3.64	4.8	70
55	800	11.4	117.7	108.3	11.98	5.4	160
55	798	12.2	118.1	109.5	11.61	5.1	160
55	800	11.2	118.7	109.6	---	5.1	140
55	600	6.2	118.1	106.7	10.45	5.0	180
55	600	6.5	117.8	106.3	10.34	4.8	160
55	400	6.6	116.8	102.1	9.34	4.8	160
55	400	6.6	116.4	101.9	8.02	4.8	150
55	200	4.5	116.4	96.6	8.35	4.9	140
55	202	4.5	116.4	95.5	---	5.8	140
54	800	8.3	143.2	143.2*	---*	10.9	50

*Hot Start Test

APPENDIX D

EXPERIMENTAL APPARATUS

EXPERIMENTAL APPARATUS

The test facilities used in this program consist of a basic vacuum system and three simple auxiliary systems for supplying heat and water for the various test units. The auxiliary systems are not operational at one time but are designed to be tied in as required by the contingencies of the test program. A major reworking of the vacuum system was required at the end of Phase III to accommodate the deterioration of performance study. This rework allowed continuous operation of the modules by adding the necessary valves and a second vacuum pump system. For the most part the test apparatus performed satisfactorily as planned. A detailed description of the equipment specifications is found in the following paragraphs and schematics (Figures 19 to 22). A photograph of the entire test facility is shown in Figure 23 and one of the electrically heated test modules set up in the vacuum chamber is shown in Figure 24.

TEST FACILITY SCHEMATICS AND SPECIFICATIONS

Vacuum System Specifications

Item 1 - Pump

Minimum requirements of 15 cfm and 50 microns dead headed pressure.

Item 2 - Glass Bell Jar

18" diameter, 30" high and clear of optical distortions.

Item 3 - Cold Trap

Liquid nitrogen cooled surface of 3 sq. ft. capable of removing 2 lb/hr of water vapor at a pressure of 50 microns for 4 hours.

Item 4 - Base Plate

20" diameter stainless steel plate equipped with vacuum tight feed throughs for electrical power, glycol, water, a pressure tap, and eight thermocouples.

Item 5 - Thermocouple Gage Transducers

0-1000 micron range, 2 required.

Item 6 - Gate Valve

6" hand gate valve, 2 required.

Item 7 - Auxiliary Vacuum System

Pump, cold trap, and thermocouple gage transducer.

WATER FEED CIRCUIT SPECIFICATIONS

Item 1 - Reservoir

6" diameter x 12" high closed stainless steel tank.

Item 2 - Sight Glass

10" long, non-corrosive fittings.

Item 4 - Filter

1/2 μ retentivity of non-corrosive material.

Item 5 - Graduated Glass Column

0-50 cc range

Item 6 - Micrometer Needle Valve

1/4" stainless steel flow control valve, 2 required.

Item 7 - Pressure Tap

Adaptable to pressure transducer over range 0-15 psia.

Item 8 - Pressure Manometer

0-50 in. Hg. range with 0.1 in. Hg. increments.

Item 9 - Needle Valves

1/4" stainless steel, 3 required.

Item 10 - Plumbing

1/4" stainless steel tubing and fittings.

AC POWER ANALYZER SPECIFICATIONSItem 1 - Powerstat

0-110 volts and 0-8 amps output and 60 cycle, 110 volt input.

Item 2 - Voltmeter

60 cycle, single phase, 0-150 volts range with 2 or 3 scales for accuracy.

Item 3 - Ammeter

60 cycle, single phase, 0-10 amp range with 2 or 3 scales for accuracy.

Item 4 - Wattmeter

60 cycle, single phase, 0-1000 watts range with 2 or 3 scales for accuracy.

GLYCOL CIRCUIT SPECIFICATIONSItem 1 - Pump

Maximum required capacity of 0.5 gpm at 20 psig.

Item 2 - Flow-meter

130-1500 ml/min range with accuracy of 1% of reading, 20 psig maximum operating pressure.

Item 3 - Temperature Control

Variable heat load to 2000 Btu/hr with regulation to prevent exceeding 250°F.

Item 4 - Micrometer Needle Valve

1/2" stainless steel

Item 5 - Needle Valves

1/2" stainless steel - standard type - 5 required.

Item 6 - Water Cooled Coil

Loop of stainless steel tubing.

Item 7 - Filter

10 micron retentivity and compatible with glycol.

Item 8 - Pressure Gage

0-25 psig range.

Item 9 - Accumulator Tank

Stainless steel construction with cover.

Item 10 - Plumbing

1/2" tubing and fittings of stainless steel or similar material which is compatible with glycol.

In addition to performance testing a brief series of bench tests were performed on each porous plate. They include a nitrogen gas flow test, a bubble point test, and a water retention test. Each test is quite simple and when used separately they provide little information. However, used collectively, they have potential value as plate acceptance tests.

The equipment used for the flow test is shown in Figure 25. It consists of a fixture to hold the test piece and a pneumatic clamping device. Two connections are provided on the fixture upstream of the porous plate, one for a regulated nitrogen supply and the other for a pressure gage. The nitrogen flow is measured with a Cox Flow rotor and the pressure is indicated on an inclined manometer. The other tests make use of the same fixture.

The bubble point test requires the cavity above the plate to be filled with a wetting fluid, usually alcohol, and the back face of the plate is pressurized with nitrogen. The bubble point is defined as that pressure at which the first bubble appears in the fluid, the location of which is generally rated.

The water retention test provides similar information to the bubble point test. Here the nitrogen connection is replaced by a water supply whose head can be closely controlled. The head is increased until the first water droplet appears on the upper surface of the plate. This is the water retention head. Each of these tests may be extended to give a qualitative indication of the distribution of the larger pores.

The electrically heated module is designed as a test unit for investigating porous plate characteristics. An assembled module is illustrated in Figure 26 and an exploded view is given in Figure 27. The objective of this type of unit was to provide a variable spacing of the water chamber, a convenient device for assembly, a uniform heat flux, and a visual observation of the water side.

The heater plate was a copper 1/8" plate with a wire resistance heater bonded to the back side. The copper plate was used so that slight variation in temperatures would tend to be minimized. The heater plate temperatures were measured by thermocouples soldered to the water side face. This was done by drilling a hole through the plate and potting a thermocouple bead flush with the inner surface.

Porous plate temperatures were measured by welding thermocouples to the porous plate with lead-ins coming through the spacer piece.

The spacer piece was made of plexiglass. Where visual observations were required, the edges were polished making the interior clearly visible when a light source was placed at side opposite the observer. The plastic stack-up imposed a temperature limitation of 150°F on the unit with an implied heat flux limitation dependent on the spacer thickness. However, the insulation characteristics of the plastic were desirable in achieving the one dimensional heated transfer that was desired.

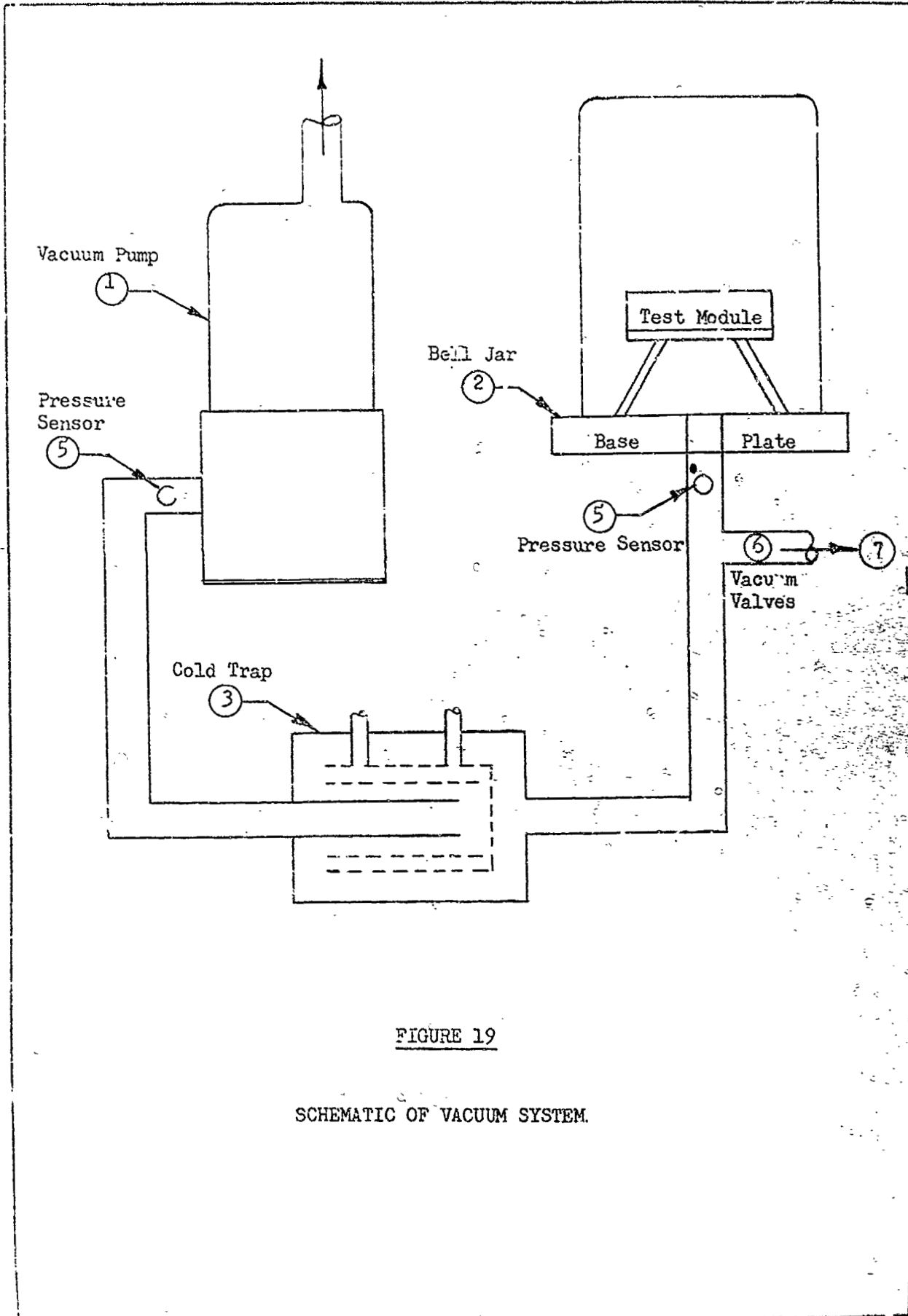


FIGURE 19

SCHEMATIC OF VACUUM SYSTEM.

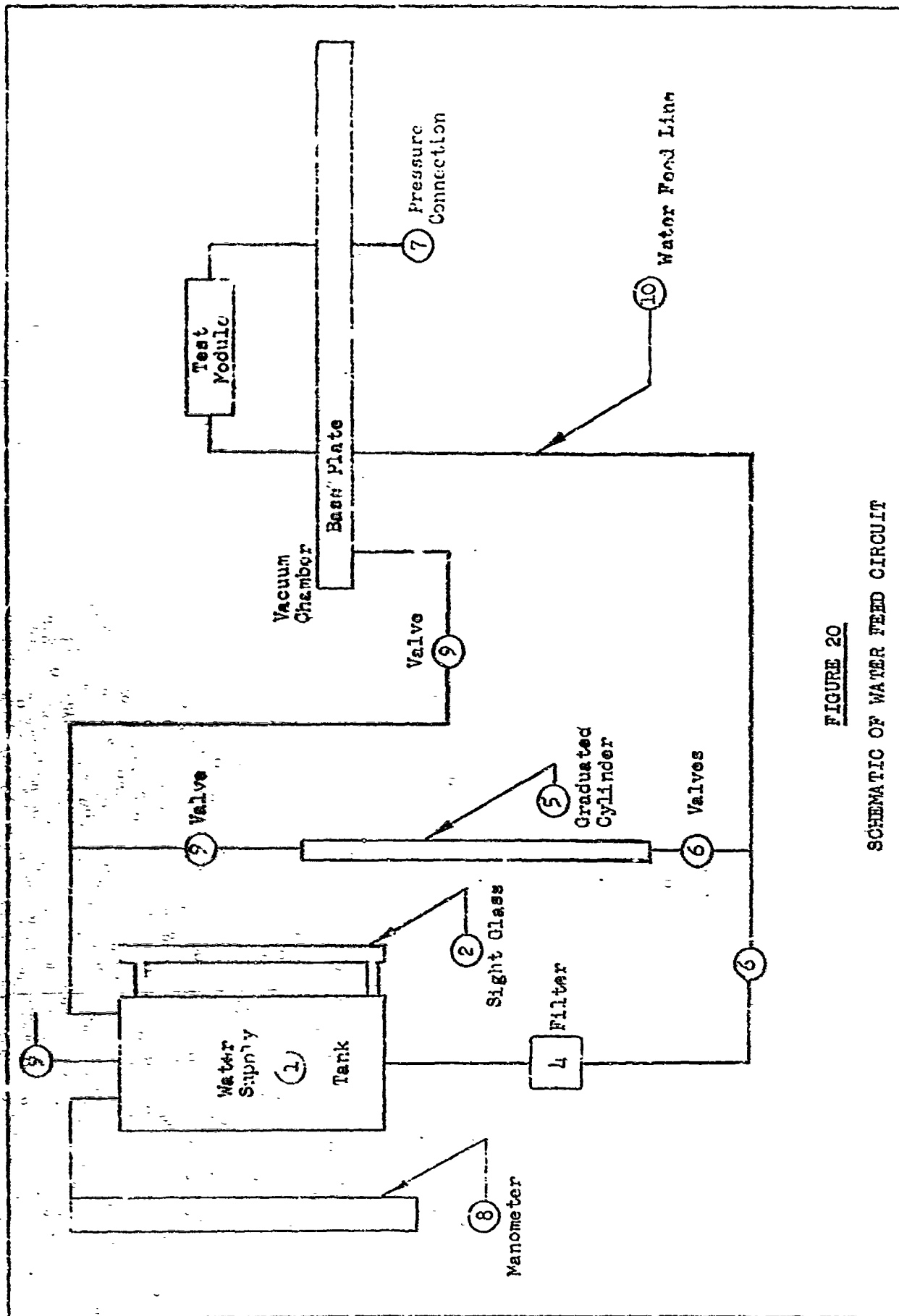


FIGURE 20
SCHEMATIC OF WATER FEED CIRCUIT

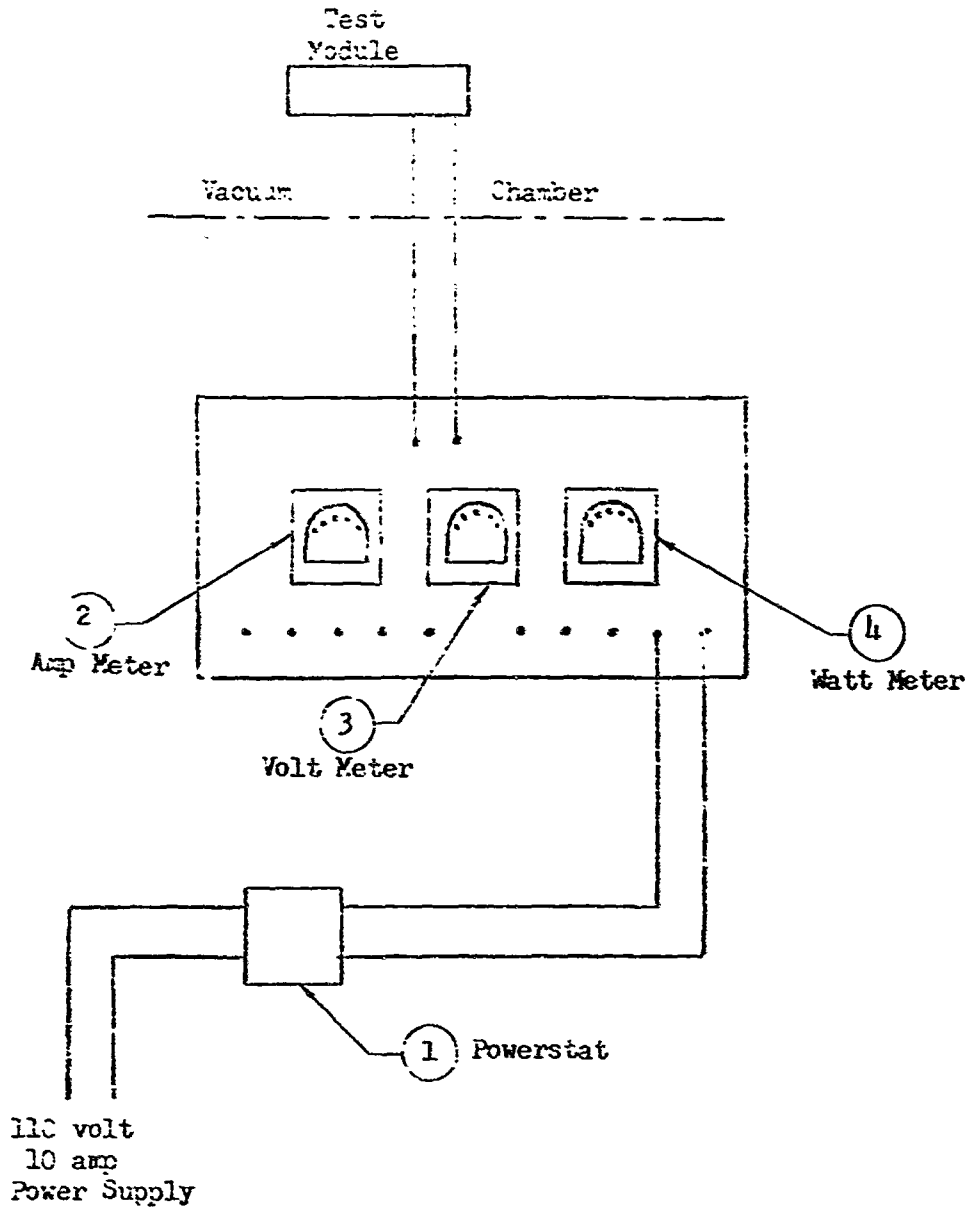


FIGURE 21

SCHEMATIC OF AC POWER ANALYZER

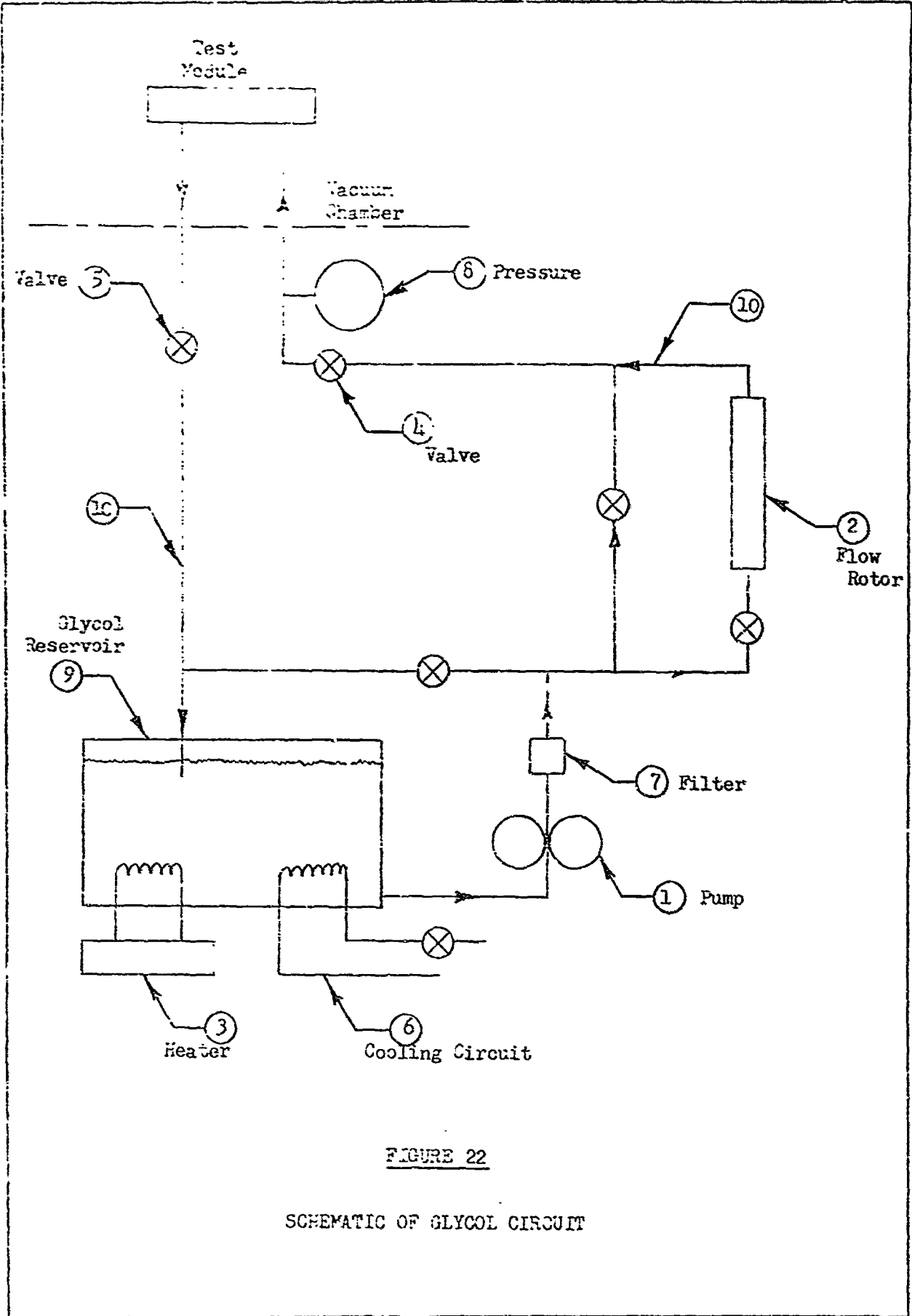


FIGURE 22

SCHEMATIC OF GLYCOL CIRCUIT

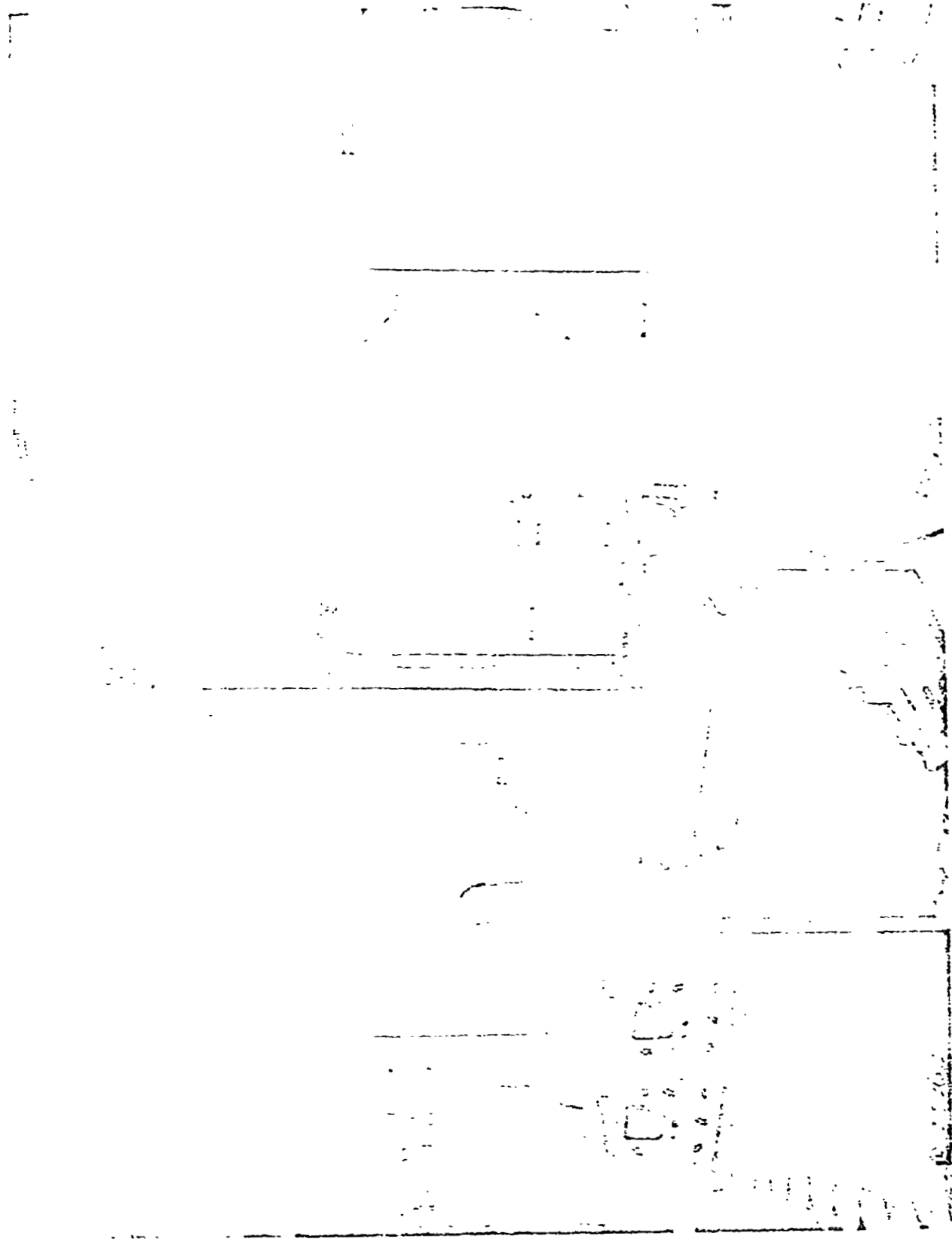


FIGURE 23 Entire Test Facility

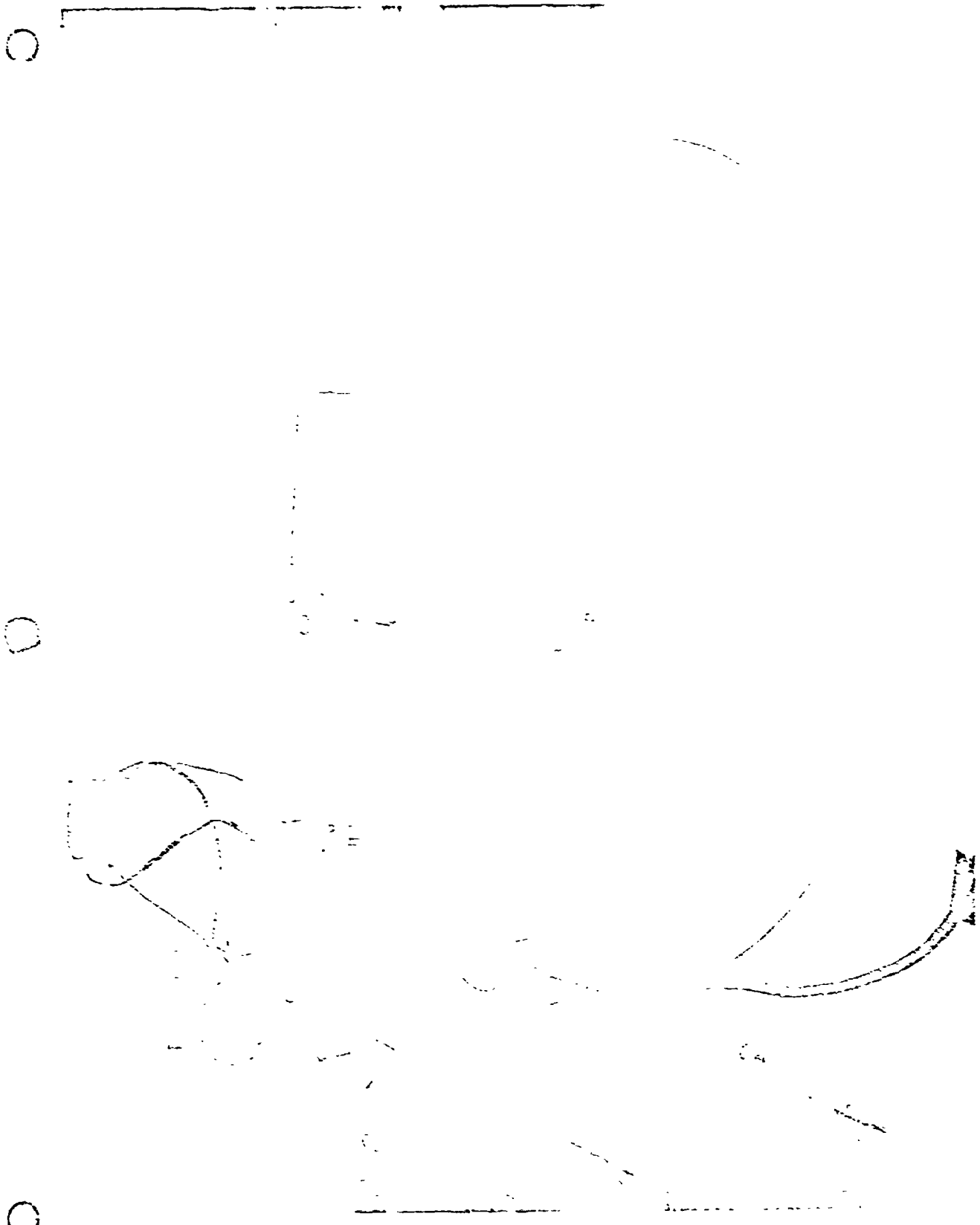


FIGURE 24 Electrically Heated Test Module Set Up in Vacuum Chamber

FIGURE 25 Apparatus for Flow Testing Porous Plates





FIGURE 26 Electrically Heated Test Module

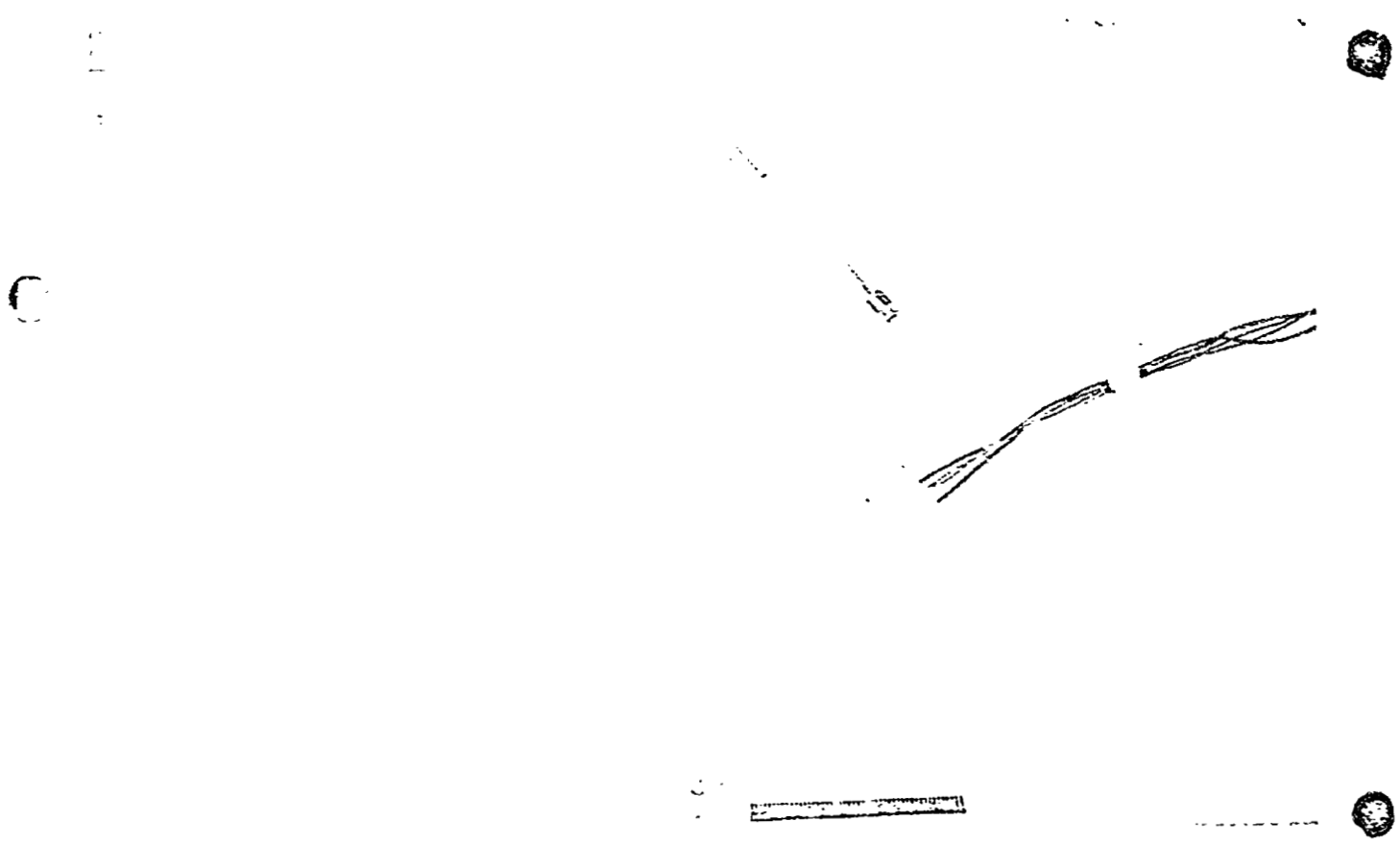


FIGURE 27 Electrically Heated Test Module - Exploded View

APPENDIX E

ANALYSIS OF THE SUBLIMATION MECHANISM WITH ENERGY TRANSFER

BY CONDUCTION AND CONVECTION

ANALYSIS OF THE SUBLIMATION MECHANISM WITH ENERGY TRANSFER

BY CONDUCTION AND CONVECTION

Considering the configuration in Figure 5, an energy balance including transfer by conduction and convection normal to the plates gives the following differential equations for the liquid and solid regions.

$$\frac{d^2 T_l}{dx^2} - \frac{C_l W}{k_l A} \frac{dT_l}{dx} = 0, \quad 0 \leq x \leq L \quad (1)$$

$$\frac{d^2 T_s}{dx^2} - \frac{C_s W}{k_s A} \frac{dT_s}{dx} = 0, \quad L \leq x \leq \delta \quad (2)$$

The general solution to this form of differential equation is simply

$$T(x) = \alpha e^{\gamma x} + \beta$$

where α and β are arbitrary constants to be evaluated from the boundary conditions, and $\gamma = \frac{C W}{k A}$ for the particular region being considered.

Evaluating the constants α and β for the following boundary conditions from Figure 5

$$T_l = T_0 \quad \text{at} \quad x = 0$$

$$T_l = T_f \quad \text{at} \quad x = L$$

$$T_s = T_f \quad \text{at} \quad x = L$$

$$T_s = T_5 \quad \text{at} \quad x = \delta$$

where T_f is the fusion temperature, the particular solutions for the liquid solid temperatures are

$$T_l(x) = T_0 - (T_0 - T_f) \cdot \left[\frac{e^{\gamma x} - 1}{e^{\gamma L} - 1} \right], \quad 0 \leq x \leq L \quad (3)$$

$$T_i(x) = T_s - (T_s - T_f) \cdot \left[\frac{e^{\gamma_i x} - e^{\gamma_i \delta}}{e^{\gamma_i L} - e^{\gamma_i L}} \right], \quad L \leq x \leq \delta \quad (4)$$

By expressing the exponentials as infinite series the relative effect of energy transfer by convection can be evaluated. The exponential series of argument y is

$$e^y = 1 + y + \frac{y^2}{2!} + \frac{y^3}{3!} + \frac{y^4}{4!} + \dots$$

Using water as the expendable coolant, as was done for this investigation, and considering a typical heat flux of 1500 Btu/hr-ft²

$$\frac{w}{A} \approx \frac{q_0/A}{h_s - h_f} \approx \frac{1500}{1050} = 1.43 \text{ lb/hr-ft}^2$$

and

$$\gamma_2 = \frac{C_2 w}{k_2 A} = \frac{1.0 (1.43)}{0.33} = 4.33 \text{ ft}^{-1}$$

$$\gamma_i = \frac{C_i w}{k_i A} = \frac{0.46 (1.43)}{1.28} = 0.514 \text{ ft}^{-1}$$

The largest plate spacing used in this program was $\delta = 0.50$ inches, which is the limiting value of x in the temperature solutions. It then follows that

$$e^{\gamma_2 x} \leq e^{\gamma_2 L} < e^{\gamma_2 \delta} = 1 + 0.1805 + \frac{(0.1805)^2}{2!} + \frac{(0.1805)^3}{3!} + \dots$$

$$e^{\gamma_i L} \leq e^{\gamma_i x} \leq e^{\gamma_i \delta} = 1 + 0.0214 + \frac{(0.0214)^2}{2!} + \frac{(0.0214)^3}{3!} + \dots$$

These simple calculations show that only the first two terms of the infinite series are significant for porous plate boiler analysis when the fluid is water and δ is less than 0.50 inches. By ignoring higher order terms of negligible magnitude the temperature solutions reduce to

$$T_1(x) = T_0 - (T_0 - T_f) \frac{x}{L}, \quad 0 \leq x \leq L \quad (5)$$

$$T_2(x) = T_s - (T_s - T_f) \left(\frac{x - \delta}{L - \delta} \right), \quad L \leq x \leq \delta \quad (6)$$

The temperature distributions are then linear for all practical purposes and energy transfer by convection can be ignored. These approximations are quite reasonable for most expendable fluids since the plate spacing used in proposed flight units is 0.075 inches.

An analysis of the sublimation mechanism for conduction heat transfer alone is presented in section 7.1. The analysis considering both convected and conducted energy transfer will be completed here.

A heat balance of the liquid layer gives

$$\frac{q_{0,2}}{A} + \frac{w}{A} C_2 T_1 = \frac{w}{A} C_2 T_f - k_2 \left. \frac{dT_2}{dx} \right|_{x=L} \quad (7)$$

or using equation (6)

$$\frac{q_{0,2}}{A} + \frac{w}{A} C_2 (T_1 - T_f) = k_2 (T_0 - T_f) \cdot \frac{e^{\frac{1}{2}L}}{e^{\frac{1}{2}L} - 1} \quad (7a)$$

where T_1 is the entering liquid temperature.

A heat balance of the solid or ice layer gives

$$h_s \frac{w}{A} + \frac{w}{A} C_i T_s = \frac{w}{A} C_i T_f - k_i \left. \frac{dT_i}{dx} \right|_{x=L} \quad (8)$$

or using equation (2)

$$h_s + C_i (T_s - T_f) \frac{\dot{w}}{A} = (T_s - T_f) k_i \gamma_i \frac{e^{\gamma_i L}}{e^{\gamma_i L} - e^{-\gamma_i L}} \quad (8a)$$

A heat balance at the liquid-solid interface gives

$$-k_s \left. \frac{dT}{dx} \right|_{x=L} + h_f \frac{\dot{w}}{A} = -k_i \left. \frac{dT}{dx} \right|_{x=L} \quad (9)$$

Equations (7), (8), and (9) can now be combined to obtain a solution for the sublimation mechanism performance. Substituting equations (7) and (8) into equation (9) gives an expression for the coolant flux in terms of the desired input heat flux and operating temperatures.

$$\frac{\dot{w}}{A} = \frac{q_o/A}{h_s - h_f - C_i (T_f - T_s) - C_e (T_i - T_f)} \quad (10)$$

Equation (8a) can be solved directly for the liquid layer thickness in terms of the coolant flux, coolant properties, plate spacing; δ , and operating temperatures.

$$L = \frac{1}{\gamma_i} \ln \left\{ \frac{[h_s - C_i (T_f - T_s)] \frac{\dot{w}}{A}}{[h_s - C_i (T_f - T_s)] \frac{\dot{w}}{A} + (T_f - T_s) k_i \gamma_i} \right\} + \delta \quad (11)$$

Finally, the performance for this mechanism can be obtained from equation (7a) as

$$T_o - T_f = \frac{e^{\gamma_i L} - 1}{k_i \gamma_i e^{\gamma_i L}} \left[\frac{q_o}{A} + \frac{\dot{w}}{A} C_e (T_i - T_f) \right] \quad (12)$$

Knowing the vapor pressure drop characteristics of a porous plate in order to obtain the sublimation temperatures; T_s , one can predict the sublimation mechanism performance of this plate by successively solving equations (10), (11) and (12). However, this procedure is considerably more complicated than the solution presented in section 7.1 which ignores the small effects of energy transfer by convection and the cooling required to reduce the supply coolant to the fusion temperature.

SYMBOLS

A	surface or face area
C	circumference or specific heat
C_g	glycol specific heat
D_h	hydraulic diameter
FPI	fins per inch
G	mass velocity
G_0	gravitational constant
H	fin height
h	heat convection coefficient
h_f	heat of fusion
h_s	heat of sublimation
I	ice layer thickness
K	constant
k	thermal conductivity
L	liquid layer thickness or fin length
l	flow length
Nu	Nusselt Number
P	Porosity
p	pressure
q	heat flux
R	gas constant
R	flow resistance
Re	Reynolds Number
T	temperature
t	porous plate thickness
tk	fin thickness

SYMBOLS (Continued)

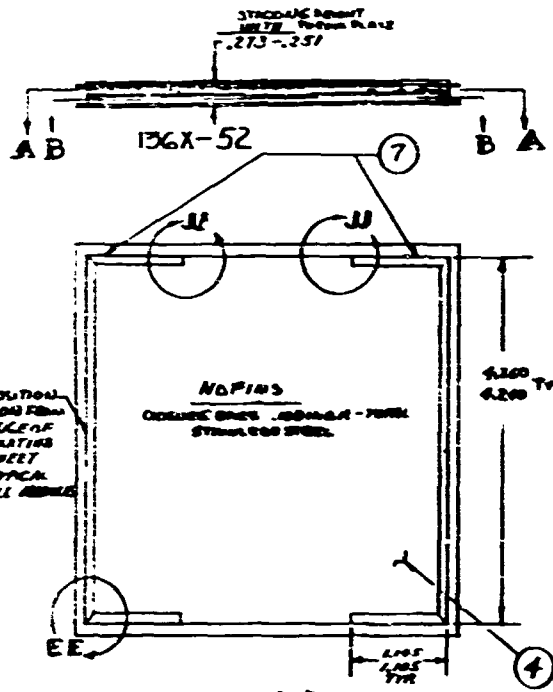
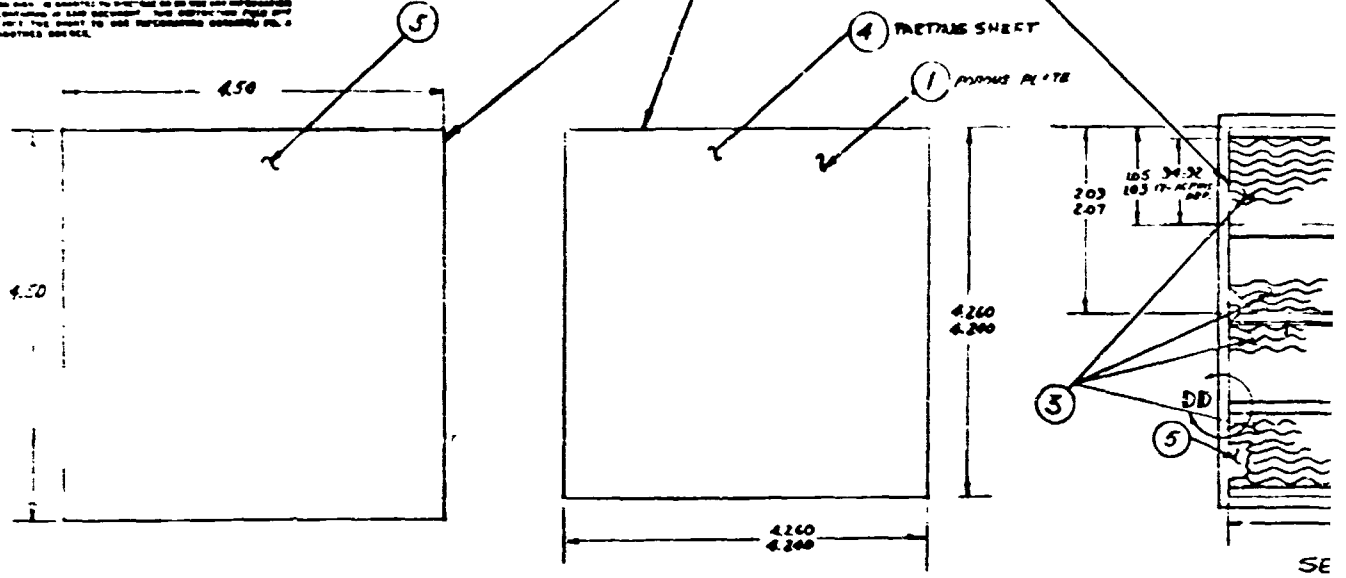
\bar{J}	equivalent thermal conductance
\bar{W}	fin width
\dot{W}	flow rate
x	distance measured from reference
ϵ	effectiveness
ϵ_s	water passage spacing
η_f	fin efficiency
η_o	overall fin efficiency
λ	molecular mean free path
μ	dynamic viscosity

SUBSCRIPTS:

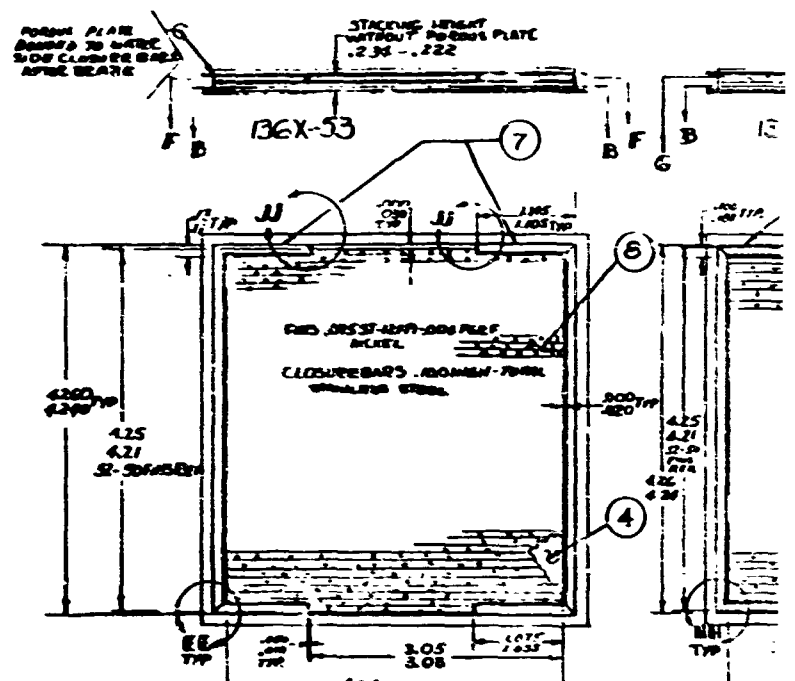
e	evaporation
eg	effective glycol side parameter
ew	effective water side parameter
f	fin
g	glycol
gi	glycol inlet
go	glycol outlet
i	ice
l	liquid
LM	log mean
m	metal
o	heated plate or surface
p or pp	porous plate
s	sublimation
ss	secondary surface
ts	total surface
w	water
1	inlet
2	outlet

REFER TO ALL DIMENSIONS UNLESS OTHERWISE SPECIFIED
 THIS DRAWING IS THE PROPERTY OF THE COMPANY AND IS NOT TO BE REPRODUCED OR TRANSMITTED IN ANY FORM OR BY ANY MEANS, ELECTRONIC OR MECHANICAL, INCLUDING PHOTOCOPYING, RECORDING, OR BY ANY INFORMATION STORAGE AND RETRIEVAL SYSTEM. THE COMPANY ASSUMES NO LIABILITY FOR DAMAGES OF ANY KIND, INCLUDING CONSEQUENTIAL DAMAGES, ARISING FROM THE USE OF THIS DRAWING. THE COMPANY ASSUMES NO LIABILITY FOR DAMAGES OF ANY KIND, INCLUDING CONSEQUENTIAL DAMAGES, ARISING FROM THE USE OF THIS DRAWING.

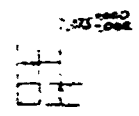
COMMON TO ALL UNITS



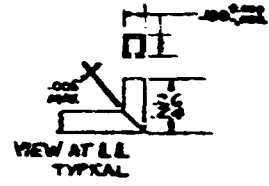
SECTION AA WATER SIDE



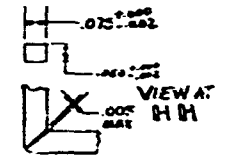
SECTION FF WATER SIDE



VIEW AT EE TYPICAL ALL CORNERS OF CLOSURE BARS



VIEW AT DD TYPICAL BOTH ENDS OF CLOSURE BARS ONE END OF FINS SEPARATORS

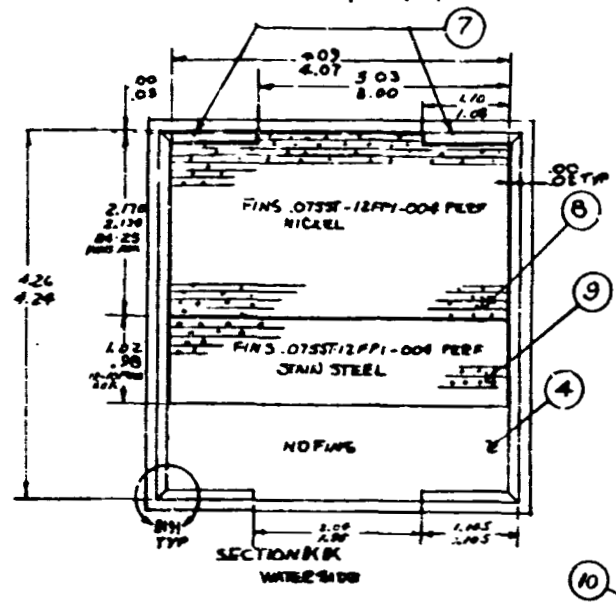
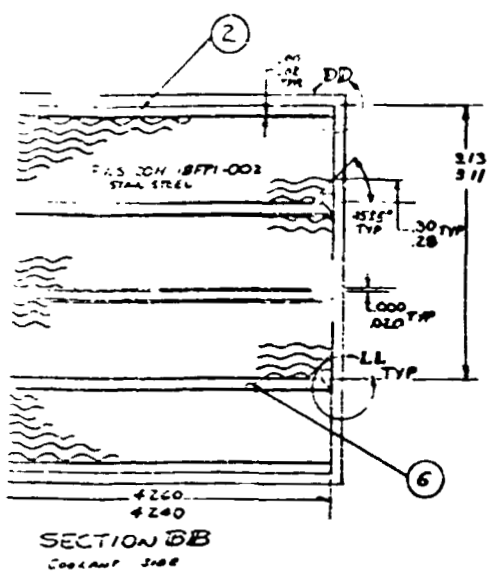


VIEW AT HH TYPICAL BOTH ENDS

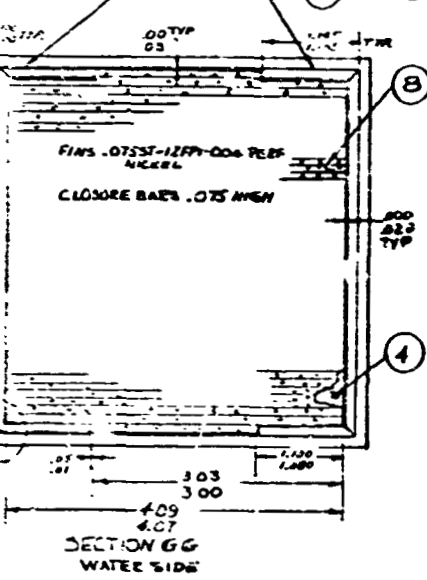
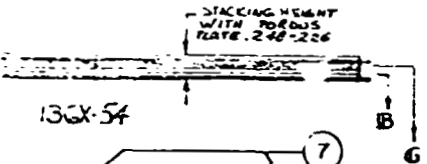
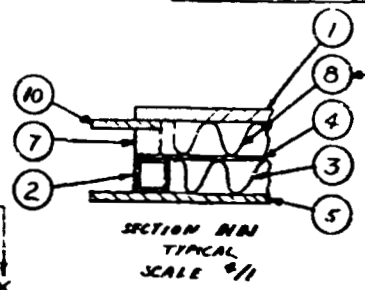
SE
 CA

1/4
 7
 5

REVISED	DATE	APPROVAL



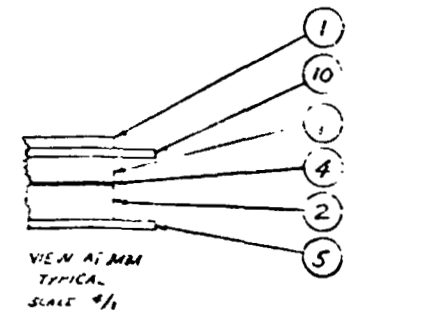
NO FIN OVER TOTAL AREA ON -SS; NO FIN OVER PORT AREA ON -SS-REF. SECTION KK



- 5 HANDLE UNIT WITH WHITE GROUTS
- 4 LEAK CHECK WATER SIDE WITH 7 P.S.G. FROM 12 DE HYDROGEN IN DRILLED WATER-ROBULANCES
- 3 SPOT WELD MIL-W-6868 CLASS C (Pb = H69)
- 2 LEAKS MAY BE REPAIRED BY WELDING MIL-W-6871 PER #5 NICKEL WELD MATL TO BE AMS 5512 OR HASTELLOY C FILLER - FLUOR PARENTAL ASPECT OF P.S.S. NOT APPLICABLE

NOTE 1 BEZEL IN VACUUM FURNACE WITH MICROBARE 20

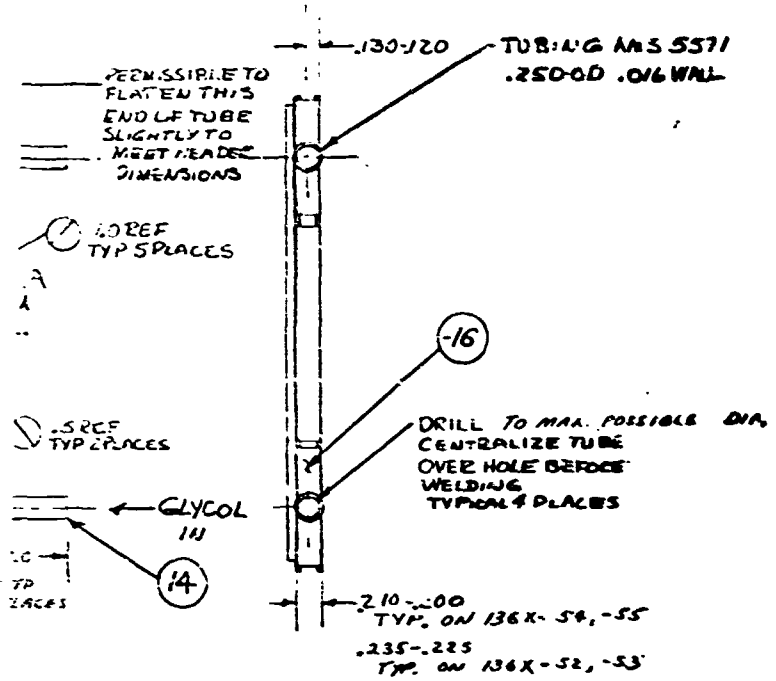
ITEM NO	NO. REQD	PART NAME	MATERIAL	REMARKS
136X-54	1	CLOSURE BAR	300X.025 ±.002	AMS 5512
136X-55-3	1	PIN WATER	STAINLESS STEEL	Q75 ST-12 FPI-004 PERE MAKE FROM 58999-1
136X-55-4	1	FIN. WATER	NICKEL	.075 3-12 FPI-004 PERE MAKE FROM 58999-1
136X-55-5	1	CLOSURE BAR	300X.025 ±.002 STAINLESS STEEL	MAKE FROM E 58999-1, 1/2" DIA. HOLE .0005 DIA. DEPTH .001
136X-55-6	1	PASS SEPARATOR	STAINLESS STEEL AMS 5537	MAKE FROM E 58999-1, 1/2" DIA. HOLE .0005 DIA. DEPTH .001
136X-55-7	1	END SHEET	STAIN STEEL .025 ±.005	AMS 5512
136X-55-8	1	PARTING SHEET	STAIN STEEL .006 ±.004	AMS 5512
136X-55-9	1	FIN. GLYCOL	STAIN STEEL 100H-18 FPI-002	MAKE FROM 58999-3 AMS 5512
136X-55-10	1	CLOSURE BAR	STAIN STEEL .008 SQ TUBING .008 WALL AMS 5511	MAKE FROM E 58999-2
136X-55-11	1	NICKEL POROUS ENDPLATE	SINTERED NICKEL POROUS PLATE	.038 MATERIAL SUPPLIED BY ENGINEERING - UNDIMED



INSPECT - TEST DESIGNATED AREAS PER		DIMENSIONS ± ANGLES ±		UNLESS OTHERWISE SPECIFIED:	
DES. (SPECIFICATIONS)		EXCEPT FOR DRILL, END FORMS, FILLET RADIUS TO SURFACES HAVING A COMMON AXIS CONCENTRIC WITHIN TIR		Δ MARK PART IDENTIFICATION: MIL-STD-130 PER HS333 IF AMING INTERPRETATION PER HS1360. CLEANING, PRESERVATION AND HANDLING PER HS1500-C.	
A	MATERIAL	DRAWN	CHECKED	Hamilton Standard	
B	ADDRESS	DRAFTING	DESIGN	WINDOR LOCKS, CONNECTICUT - U.S.A.	
C	HEAT TREAT SPEC	MATERIALS	PROJECT COST FACTORY	POROUS PLATE MODULES	
ALL AREAS	SURFACE COATING	PRELIM PROO	PROO	CODE IDENT NO	SIZE
ALL AREAS	INFO SPEC			73030 D	136X-52-55
ALL AREAS	MAKE FROM			SCALE: 1/4" = 1"	WEIGHT: LB SHEET 1 OF 2
ALL AREAS	PROD. CODE				

SYM	DESC.	DATE	APPROVAL

HEADER
JING



136X 52 → 55

NOTES

- ALL HEADER MATERIAL AMS 5572
- PRESSURE TEST GLYCOL SIDE 25 PSIG UNDER WATER - NO BUBBLES
- USE NITROGEN OR FREON-12 & DISTILLED WATER FOR TEST
- HANDLE UNIT WITH WHITE GLOVES AT ALL TIMES
- THIS DRAWING APPLICABLE TO 136X-52-53-54 & 55

EST. NO.		UNLESS OTHERWISE SPECIFIED:		DRAWN		Hamilton Standard		U	
REV.		DIMENSIONS ± — ANGLES ± —		H Smith		WINDSOR LOCKS, CONNECTICUT • U.S.A.		A	
DESCRIPTION(S)		EXCEPT FOR DRILL END FORMS, FILLET RADIUS TO SURFACES HAVING A COMMON AXIS CONCENTRIC WITHIN TIR.		S/MS		PROJECT		APPLICATION	
MATERIAL		MATERIALS		COST		FACTORY		CODE IDENT NO	
HARDNESS		PROJECT		EXP MFG		RELIM PROD		SIZE	
HEAT TREAT SPEC		FACTORY		PROD.		73030		C	
SURFACE COATING		EXP MFG		RELIM PROD		PROD.		136X-52 → 55	
MFG SPEC		EXP MFG		RELIM PROD		PROD.		SCALE: <i>None</i>	
MAKE FROM		EXP MFG		RELIM PROD		PROD.		WEIGHT:	
PROD. CODE		EXP MFG		RELIM PROD		PROD.		LB SHEET 2 OF 2	

A